

BRIDGE LOAD RATING USING DYNAMIC RESPONSE COLLECTED THROUGH  
WIRELESS SENSOR NETWORKS

by

Amer Shamil Jaroo

Submitted in Partial Fulfillment of the Requirement

for the Degree of

Master of Science in Engineering

in the

Civil and Environmental Engineering

Program

YOUNGSTOWN STATE UNIVERSITY

December, 2013

Bridge Load Rating Using Dynamic Response Collected Through Wireless Sensor  
Networks

Amer Shamil Jaroo

I hereby release this dissertation to the public. I understand that this dissertation will be made available from the OhioLINK ETD Center and the Maag Library Circulation Desk for public access. I also authorize the University or other individuals to make copies of this dissertation as needed for scholarly research.

Signature:

---

*Amer Shamil Jaroo*, Student Date

Approvals:

---

*Dr. AKM Anwarul Islam, P.E.* Date  
Thesis Advisor

---

*Dr. Javed Alam*, Committee Member Date

---

*Dr. Frank Li*, Committee Member Date

---

*Dr. Sal Sanders* Date  
Associate Dean, School of Graduate Studies and Research

## ABSTRACT

This paper describes a method for load rating of prestressed box beam (PSBB) bridges based on their dynamic response collected using wireless sensor networks (WSNs). Although the percentage of deficient bridges in the United States has been declining slowly, a significant portion is still closed to traffic or posted with load restrictions. An accurate load rating of bridges is very expensive; therefore, new tools for quick, efficient and response-based load rating of bridges will save time and money. The hypothesis is based on the assumption that the health of a bridge is associated with its vibration signatures under vehicular loads. Two WSNs were deployed on a 25-year old PSBB bridge under trucks with variable loads and speeds for collecting real-time dynamic response at the current condition. Dynamic simulations of three dimensional finite element models of a bridge were performed to acquire its dynamic response under vehicular loads at its newest condition right after construction. The bridge model was validated by field testing and numerical analysis. Fast Fourier Transform and peak-picking algorithms were used to find maximum peak amplitudes and their corresponding frequencies. This information and the necessary bridge geometric parameters were used to calculate the in-service stiffness of the bridge in order to develop application software for load rating of bridges. The application software can instantly calculate the load rating of a PSBB bridge by collecting its real time dynamic response under vehicular loads using WSNs. The research outcome and the software will help reduce bridge maintenance costs and will increase public safety.

**Keywords:** Prestressed box beam bridge, bridge load rating software, health monitoring of bridges, wireless sensor network, bridge maintenance.

## **ACKNOWLEDGEMENTS**

This research would not have been possible without the help and support of many people. First and foremost, I would like to express gratitude towards my supervisor, Dr. AKM Anwarul Islam, P.E., who has supported me throughout my thesis with his patience and knowledge. Also, I would like to thank him for giving me the opportunity to work with him in this ODOT funded research. I would like to thank the committee members, Drs. Javed Alam, and Frank Li, for serving on my thesis defense committee and helping me in various ways during performing this research. I would also like to thank Mr. John P. Picuri, P.E., Project Manager, ODOT District 4 Planning and Engineering, and the personnel at the Engineer's Offices in Mahoning, Ashtabula and Trumbull County, and Ohio Highway Patrol for their help and support. I would like to extend my gratitude to the Higher Committee for Education Development in Iraq for their support through the HCED scholarship program. Finally, I am deeply thankful to my parents, family members, and friends for their inspiration and support.

# TABLE OF CONTENTS

ABSTRACT.....	iii
ACKNOWLEDGEMENTS.....	iv
TABLE OF CONTENTS.....	v
LIST OF FIGURES .....	viii
LIST OF TABLES .....	x
1. Introduction and Literature Reviews .....	1
1.1 General Overview .....	1
1.2 Problem Statement.....	2
1.3 Load Rating of Bridges.....	5
1.4 Research Objectives.....	6
1.5 Literature Reviews .....	8
2. Field Investigations.....	13
2.1 Bridge Selection.....	13
2.2 SunSPOT Sensors and WSN .....	15
2.3 Moving Loads on Bridges.....	17
2.4 WSN Setup and Data Collection.....	18
2.4.1 WSN Setup.....	18
2.4.2 Sensors and Truck Locations .....	20
2.4.3 Acceleration Data Collection.....	21
3. Modeling and Simulation.....	24
3.1 Finite Element Modeling .....	24

3.2	Bridge Descriptions .....	24
3.3	FE Modeling of ATB Bridge .....	26
3.3.1	Creating Model Parts .....	26
3.3.2	Defining Part Properties.....	27
3.3.3	Creating Model Assembly .....	28
3.4	Load Generation.....	30
3.5	Bridge Model Analysis .....	31
3.5.1	Static and Dynamic Analyses .....	31
3.5.2	Frequency Analysis.....	34
3.6	FE Model Validation.....	35
4.	Bridge Load Rating.....	38
4.1	Equation of Motion and Natural Frequency .....	38
4.2	Bridge Response Analysis .....	40
4.3	Load Rating Methodology .....	45
4.3.1	ATB Bridge Fundamental Frequency.....	45
4.3.2	Idealized Bridge and Load Rating Equations .....	47
4.4	Load Rating of ATB Bridge .....	50
4.5	Load Rating Flow Chart.....	52
4.6	Application Software and Validation.....	57
5.	Conclusions and Recommendations .....	61
5.1	Conclusions.....	61
5.2	Recommendations.....	62

6. REFERENCES.....	64
7. APPENDICES .....	68
Appendix A.....	68
Appendix B.....	75
Appendix C.....	82
Appendix D.....	85

## LIST OF FIGURES

Figure 1-1: Bridge behavior as an elastic spring. ....	10
Figure 2-1: MAH Bridge. ....	15
Figure 2-2: ATB Bridge.....	15
Figure 2-3: SunSPOT hardware kit.....	16
Figure 2-4: Internal parts of SunSPOT sensor and base station. ....	17
Figure 2-5: Recording truck axle dimensions and weights.....	18
Figure 2-6: Configuration of two WSNs used on bridges. ....	19
Figure 2-7: SunSPOT sensors with external battery.....	20
Figure 2-8: Graphical representation of truck path and sensor locations. ....	21
Figure 2-9: Field data collection. ....	21
Figure 2-10: Acceleration of ATB Bridge in time domain.....	23
Figure 3-1: A typical PSBB cross-section of ATB Bridge.....	25
Figure 3-2: ATB Bridge PSBB layout plan. ....	25
Figure 3-3: ATB Bridge cross-section.....	26
Figure 3-4: Parts of ATB Bridge model. ....	27
Figure 3-5: ATB Bridge: assembly model.....	29
Figure 3-6: ATB Bridge model: sensor locations and boundary conditions. ....	31
Figure 3-7: Prestress effect on ATB Bridge model (exaggerated). ....	32
Figure 3-8: Acceleration of ATB Bridge model in time domain.....	33
Figure 3-9: Vibration mode shapes of ATB Bridge model.....	34
Figure 3-10: ATB Bridge model validation: static analysis. ....	35
Figure 3-11: ATB Bridge model validation: frequency analysis.....	37



Figure 4-1: SDOF spring- mass system. ....	39
Figure 4-2: Amplitude vs. frequency data of ATB Bridge. ....	41
Figure 4-3: Amplitude vs. frequency data of ATB Bridge model. ....	44
Figure 4-4: ATB Bridge model: mode shape under vehicular loads. ....	46
Figure 4-5: Beam with fixed end supports. ....	47
Figure 4-6: Bridge geometric properties. ....	53
Figure 4-7: Load rating input page. ....	54
Figure 4-8: Load rating flow chart. ....	55
Figure 4-9: Load rating flow chart (continued). ....	56
Figure 4-10: Input Parameters tab of ODOTApp application software. ....	57
Figure 4-11: Bridge Assessment output tab of ODOTApp application software. ....	58
Figure 4-12: Input Parameters tab of ODOTApp with TRU Bridge response. ....	59
Figure 4-13: Bridge Assessment tab of ODOTApp with TRU Bridge response. ....	60

## LIST OF TABLES

Table 1-1: Conditions of highway bridges in U.S. (2005-2012) .....	2
Table 1-2: Numbers of deficient bridges in rural and urban areas .....	4
Table 1-3: Bridge postings (2007 – 2012) .....	4
Table 2-1: List of bridges proposed to ODOT for data collection.....	14
Table 3-1: Material properties of elements in ATB Bridge model.....	28
Table 3-2: Comparisons of FE model and hand calculations .....	36
Table 4-1: ATB Bridge peak amplitude.....	42
Table 4-2: ATB Bridge frequency at most dominant peak.....	42
Table 4-3: ATB Bridge model peak amplitude.....	43
Table 4-4: ATB Bridge model frequency at most dominant peak.....	43
Table 4-5: ATB Bridge model: FFT results for displacement data .....	46
Table 4-6: ATB Bridge load rating for different trucks.....	51
Table 4-7: Load rating of ATB Bridge using BARS and VIRTIS .....	52
Table 4-8: Ohio legal load vehicles weight and load configuration. ....	52

# CHAPTER 1

## Introduction and Literature Reviews

### 1.1 General Overview

The majority of bridges in the United States were built to last around fifty years; however, their current average age is 42 years (ASCE, 2013). During their service life, the performance of bridges is compromised due to various reasons including corrosion in reinforcement, reduction in concrete strength, fatigue cracks in steel, cracks in concrete, etc. As a result, the load bearing capacity of bridges decreases over time. The load rating is usually defined as the service live load that can be carried safely over a bridge, and is expressed as a rating factor (RF) or in terms of tonnage for a particular vehicle. Load and resistance factor rating (LRFR) and load factor rating (LFR) are commonly used methods to perform load rating of bridges to ensure public safety. These methods are recommended by the American Association of State Highway and Transportation Officials (AASHTO), and used by the Ohio Department of Transportation (ODOT) and other state Departments of Transportation (DOTs). However, it has been found that bridges typically have higher capacity in comparison to their theoretical strength (Lichtenstein, 1993). The current theoretical load rating of bridges is a very conservative approach and sometimes proposes capacity well below the actual strength because of factors, such as loss in material strength over time, changes in load distribution characteristics, and unaccounted non-structural components. These factors contribute to the structural response of a bridge and its load rating. Therefore, this research is aimed at developing a new method to estimate the load rating of bridges by collecting and

analyzing their real-time dynamic structural response. This method will be able to estimate the load bearing capacity of a bridge and may avoid over-conservative evaluation. Moreover, there will be a reduction in maintenance costs as a result of this cost-effective solution.

## 1.2 Problem Statement

According to the U.S. Department of Transportation (USDOT), of around 607,380 bridges across the country, 151,497 (24.9%) were categorized as deficient bridges [66,749 (11%) as structurally deficient and 84,748 (14%) as functionally obsolete] as shown in Table 1-1 and stated in the “Report Card for America’s Infrastructure” published by the American Society of Civil Engineers (ASCE, 2013). Structurally deficient bridges are not unsafe, but they must be posted for speed and weight limits because of limited structural capacity. Functionally obsolete bridges have older design features and geometrics, and although not unsafe, they cannot accommodate current traffic volumes, vehicle sizes, and weights.

Table 1-1: Conditions of highway bridges in U.S. (2005-2012)

Year	Structurally deficient	Functionally obsolete	Total
2012	66,749	84,748	151,497
2011	68,759	84,832	153,591
2010	70,431	85,858	156,289
2009	72,402	87,460	159,862
2008	71,469	89,189	162,072
2007	72,066	89,080	163,146
2006	75,422	89,591	165,013
2005	77,863	90,010	167,873

From 2001–2011, the number of structurally deficient plus functionally obsolete bridges in rural areas declined by 24,723. However, in urban areas during the same time frame, the number increased by 3,577. In 2008, approximately one in four rural bridges was deficient, while in urban areas, the ratio was one in three. Numbers of structurally deficient and functionally obsolete bridges in rural and urban areas from 2001 to 2011 are shown in Table 1-2 (USDOT, 2012). In addition to the overall reduction in the number of deficient bridges, the percentage of postings on the nation’s bridges has also declined gradually over the past five years. On the other hand, the number of bridges closed to traffic has climbed from 2,816 in 2007 to 3,585 in 2012, and during the same time frame, the number of bridges posted for load restrictions has decreased from 67,969 to 60,971, as shown in Table 1-3 (ASCE, 2013). Posted bridges do not necessarily threaten public safety, but they can create traffic congestion, and force emergency vehicles and trucks to take lengthy detours when a bridge is closed. It was estimated in 2008 that it would cost roughly \$140 billion to repair every deficient bridge in the country – about \$48 billion to repair structurally deficient bridges and \$92 billion to improve functionally obsolete bridges (AASHTO, 2008). According to the National Surface Transportation Policy (NTSP) report, it will cost roughly \$850 billion to eliminate all existing bridge deficiencies as they arise over the next 50 years. This equates to an average annual investment of \$17 billion (NSTP, 2007).

Table 1-2: Numbers of deficient bridges in rural and urban areas

Year	2001	2003	2005	2007	2009	2011
All bridges	589,685	591,940	590,553	599,766	603,259	630,141
Urban	133,401 22.62%	135,415 22.88%	137,598 23.30%	151,171 25.20%	156,305 25.91%	183,918 29.19%
Rural	456,284 77.38%	456,525 77.12%	452,955 76.70%	448,595 74.80%	446,954 74.09%	446,223 70.81%
Structurally deficient bridges, total	83,595 14.18%	79,775 13.48%	75,923 12.86%	72,520 12.09%	71,177 11.80%	67,522 10.72%
Urban	12,705 15.20%	12,316 15.44%	12,600 16.60%	12,951 17.86%	12,828 18.02%	11,923 17.66%
Rural	70,890 84.80%	67,459 84.56%	63,323 83.40%	59,569 82.14%	58,349 81.98%	55,599 82.34%
Functionally obsolete bridges, total	81,439 13.81%	80,990 13.68%	80,412 13.62%	79,804 13.31%	78,477 13.01%	76,366 12.12%
Urban	29,383 36.08%	29,886 36.90%	31,391 39.04%	33,139 41.53%	33,743 43.00%	33,742 44.18%
Rural	52,056 63.92%	51,104 63.10%	49,021 60.96%	46,665 58.47%	44,734 57.00%	42,624 55.82%

Table 1-3: Bridge postings (2007 – 2012)

Year	2007	2008	2009	2010	2011	2012
Closed to all traffic	2816	2,966	3,552	3,538	3,578	3,585
Posted for load	67969	66,052	66,249	63,072	61,575	60,971
Posted for other load-capacity restriction	2559	2,529	2,669	2,953	2,916	3,040
Total	73,344 (12.3%)	71,547 (11.9%)	72,470 (12.0%)	69,563 (11.5%)	68,069 (11.25%)	67,596 (11.1%)

The AASHTO Bridge Analysis and Rating System (BARS) software has been used since the early eighties for theoretical load rating of bridges. BARS software, which uses the LFR approach, appears to be inappropriate in rating bridges designed using the Load and Resistance Factor Design (LRFD) method. However, AASHTO has developed a new load rating software called VIRTIS that uses the LRFR approach. Although there is an increased emphasis on using LRFR over LFR, neither method, in fact, reveals hidden structural damage and/or deteriorations. As a result, realistic bridge load ratings are not available from either of the AASHTO software. On the other hand, traditional wired sensor networks for health monitoring of large civil structures require large amounts of coaxial cables that are expensive to install and maintain. With the advancement in wireless communication technology, use of wireless sensors in structural health monitoring has become an effective and dominant choice to reduce cost, and increase convenience and public safety.

Table 1-2 shows that a large amount of the nation's bridges is structurally deficient or functionally obsolete. In addition, Table 1-3 shows that 11.1% of the nation's bridges is closed to traffic or posted for load restrictions. Therefore, it is important to develop response-based methods and tools to estimate load rating of bridges that will provide more realistic results. The outcome of this research will be useful for ODOT and other state DOTs in load rating of highway bridges.

### **1.3 Load Rating of Bridges**

According to the current data of deficient bridges in the state and highway systems, out of 27,045 bridges across the State of Ohio, 6,773 (25%) were categorized as deficient bridges [2,462 (9.1%) as structurally deficient and 4,311 (16%) as functionally

obsolete] (USDOT, 2012). ODOT has its own Manual for Bridge Inspection (MBI), which is used for bridge inspections in the State of Ohio to ensure public safety. Different types of inspection with diverse scope, intensity and frequency have been suggested in the MBI. Five general types among those are: Initial Inspection, Routine Inspection, Damage Inspection, In-Depth Inspection, and Special Inspection (ODOT MBI, 2010).

The bridge load rating is performed in two of these five inspection types. During the Routine Inspection, the load rating might be performed to determine the need for establishing or revising a weight restriction on the bridge (ODOT MBI, 2010). On the other hand, the In-Depth Inspection might require a structural analysis for load bearing capacity to ensure the safety of one or more members and to distinguish any deficiency not easily determined using Routine Inspection (ODOT MBI, 2010). Procedures, guidelines and policies for determining the safe live load bearing capacity of highway bridges in the State of Ohio were mentioned in the ODOT Bridge Design Manual (ODOT BDM, 2007).

#### **1.4 Research Objectives**

The prestressed box beam (PSBB) bridges constitute about 17 percent of bridges built annually on public roads according to the recent National Bridge Inventory (NBI) data (NCHRP, 2008). These bridges are widely used and have many advantages over other types of bridges in speed and ease of construction, aesthetics, span-to-depth ratio and cost. Although early construction practices might have led to serviceability issues, improved practices have made the PSBB bridge a viable and cost-effective choice (PCI, 2011). The span limit for PSBB bridges usually ranges from 15 to 100 ft, but span lengths up to 120 ft have been designed and constructed. This type of bridge is not



normally used for four-lane divided highways or where the one-way design average daily truck traffic (ADTT) exceeds 2,500 (ODOT, 2011). The objective of this research is to develop methods and tools for load rating of a PSBB bridge under vehicular loads by analyzing its real-time dynamic response collected through WSNs. The hypothesis is based on the assumption that the health of a bridge is associated with its vibration signatures under vehicular loads. Therefore, the load bearing capacity of a bridge can be estimated from the analysis of its dynamic response, such as acceleration, under moving loads. The load rating of a bridge is usually estimated theoretically using software, and sometimes performed using a real truck on the bridge, which is very expensive. Often times the theoretical method is inadequate, or perhaps inefficient, from a global perspective of unseen bridge deterioration over the years due to vehicular and environmental distresses. A novel approach of estimating the load bearing capacity of bridges studied herein can be very useful and cost-efficient.

Many of the damage detection algorithms that have been reported by the structural engineering community typically consider changes in global structural vibration characteristics as indicators of damage and deterioration of a bridge. The goal of this research is load rating of a bridge using WSN. In pursuit of this goal, a 25-year old single-span PSBB bridge in Ohio was equipped with two sets of WSN for collecting real-time acceleration data under trucks with various speeds and weights. Also, the dynamic response of the bridge at its newest condition (right after construction) was collected from analytical simulations of its three dimensional finite element (FE) models. Fast Fourier Transform and peak picking algorithms were used to analyze the dynamic response data from the field and FE bridge model. The bending stiffness of the bridge in

the current condition was calculated using the analysis data along with the bridge geometric parameters. Using the load displacement relationship and the calculated bending stiffness, bridge load bearing capacity was estimated.

The application software developed from this research will be able to promptly estimate the load rating of other single-span PSBB bridges by collecting their real-time dynamic response. This novel technique may fundamentally change the current theoretical approach of bridge load rating. This application software is expected to help ODOT save time and money for bridge maintenance to ensure public safety.

## **1.5 Literature Reviews**

The structural health monitoring (SHM) consists of a system that has the ability to evaluate conditions of a structure and detect changes in the structural performance over time. There are many applications of SHM in various fields, mainly in aerospace and civil engineering (Balageas, *et al.*, 2006). The use of traditional wired sensor networks for the health monitoring of large civil structures requires large amounts of coaxial cables that are expensive to install and maintain. Therefore, WSN is expected to be a cost-effective and efficient choice over tethered networks for the health monitoring of highway bridges.

Wireless sensor networks have been used by many researchers for health monitoring of structures. Straser and Kiremidjian (1998) first proposed the integration of wireless communication technology with sensors as a tool for real-time condition assessments of civil infrastructures due to long-term deterioration or effects of extreme events, such as earthquakes. Kim, *et al.* (2007) deployed a 64-node wireless sensor

network on the 4,200 ft long main span of the Golden Gate Bridge in San Francisco. The goal was to identify initial issues with WSN in SHM and to monitor ambient vibrations at a low cost without interrupting the daily operation of the bridge. Gangone, *et al.* (2008) deployed a 20-node WSN in Potsdam, New York, which also supported strain gages apart from accelerometers. The data collected using the WSN in both efforts were able to capture important modes of dynamic bridge behavior, which agreed with the theoretical results.

Bridges are vital elements in a transportation network because they control the capacity of the system by controlling the volume and weight of traffic that can be carried over the system. Besides, the construction and maintenance cost per mile for bridges is the highest in a transportation network (Barker, 2007). Therefore, extensive research has been performed to study and evaluate the load capacity and safety of highway bridges.

The load rating of bridges has been studied by many researchers. Some of them have focused on using the dynamic response of bridges to estimate their in-service stiffness and load bearing capacity. The main goal of Chen, *et al.* (2002) was to develop a new method to perform load rating of bridges. The researchers used the ambient vibration measurement technology, which assumed that a bridge behaves like an elastic spring, as shown in Fig. 1-1, and the load capacity of a bridge is directly related to the stiffness of the spring. By knowing the vibration frequency,  $f$ , and mass,  $m$ , of the bridge, the flexural stiffness,  $K$ , of the bridge can be calculated by using Eq. 1.1. Due to the deterioration of materials and loss of structural integrity over time, the stiffness of a structure decreases over time. In other words, a bridge will be more flexible and have a lower frequency of

vibration. The reduced stiffness of the old bridge,  $\tilde{K}$ , can also be calculated using Eq. 1.1, and the change in stiffness ( $\Delta K = K - \tilde{K}$ ) can be determined as well.

$$K = f^2 * m \quad (1.1)$$

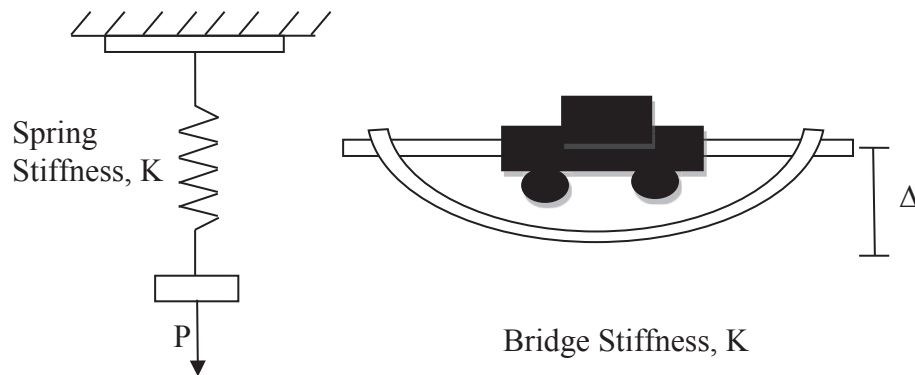


Figure 1-1: Bridge behavior as an elastic spring.

In order to verify this method, Chen, *et al.* (2002) constructed a miniature bridge model, which consisted of four plastic girders that were bonded to a Plexiglas deck with a 20-degree skew. Both static and dynamic tests were performed on the miniature bridge model. After a cut through the mid-span, static and dynamic tests were repeated to simulate the deterioration in the miniature bridge model. A finite element (FE) model was also created using ALGOR to verify the results from the miniature bridge model tests.

Samali, *et al.* (2003) found a new, simple, non-expensive, and safe procedure to determine the load bearing capacity of short-span timber bridges. They attached highly sensitive accelerometers underneath the bridge and used a model impact hammer bridge excitation. The dynamic response of the bridge was recorded in two cases: (1) with an extra load applied at the bridge mid-span, and (2) without any external load on the bridge.

From the bridge response, the first natural frequencies,  $\omega_1$  and  $\omega_2$  for cases (1) and (2), respectively, were determined. By knowing the added weight,  $\Delta M$ , the flexural stiffness,  $K$ , of the bridge can be calculated using Eq. 1.2.

$$K = \frac{\omega_1^2 * \omega_2^2}{\omega_1^2 - \omega_2^2} * \Delta M \quad (1.2)$$

The load bearing capacity was estimated from the relationship between the actual measured stiffness,  $EI$ , and the bending capacity of timber. This relationship was derived by incorporating the uncertainties of the geometric properties and full-scale tests based strength properties of some 1,200 round timber poles.

Chowdhury (1999) proposed a nondestructive dynamic method to estimate the load capacity of beams. This method included a shaker to excite the beams and to record three forced responses, such as displacement, velocity, and acceleration, using four different types of sensors to measure the effectiveness of each sensor. The dynamic responses of beams were analyzed to estimate their static stiffness. The calculated stiffness of beams was used to estimate their load bearing capacity using load displacement relationship. For example, the load bearing capacity of a beam with deflection limited to  $L/400$  was calculated using Eq. 1.3.

$$\text{Load Bearing Capacity} = K * \frac{L}{400} \quad (1.3)$$

Chowdhury concluded that the proposed method can estimate the bending stiffness of a beam. Also, the researcher stated that the measured stiffness is a sensitive indicator of physical changes, which can be used for monitoring bridge performances during its service life.

In all of the above mentioned efforts, the target of the researchers was to find a method for load capacity prediction using the dynamic response data for the structures. All of the methods used the dynamic response to find the stiffness of the structures, and used the calculated stiffness to determine their load bearing capacity. Both Chowdhury (1999) and Chen, *et al.* (2002) found the stiffness of the tested structures using the generalized single degree of freedom (SDOF) method. While Samali, *et al.* (2003) found the stiffness using the first natural frequencies of the dynamic response, as stated in Eq. 1.2. All of the previous researchers mentioned the possibility of using the force displacement relationship in Eq. 1.3 to calculate the load bearing capacity of a structure after estimating its bending stiffness. The proposed load rating method in this research includes analysis of dynamic response of single span PSBB bridges in order to find the maximum peak amplitudes and their corresponding frequencies. Using the SDOF method and the analysis data, the bending stiffness of a bridge can be determined. By using the force displacement relationship, the load bearing capacity of bridges can be estimated as well within an acceptable accuracy.

## CHAPTER 2

### Field Investigations

#### 2.1 Bridge Selection

The objective of this research is to develop a tool for load rating of PSBB bridges by analyzing their dynamic response under vehicular loads collected through wireless sensor networks. Three PSBB bridges were selected for this study. Two of them were used for data collection and modeling. The third one was used to validate the application software developed based on the response from the first two bridges. Following points were taken into consideration during the final selection of the bridges:

1. Single-span bridges were selected for ease of modeling and simulation.
2. Bridges with low average daily traffic (ADT) were preferred to minimize traffic disruption during data collection.
3. At least two relatively older bridges were selected to ensure the presence of sufficient deterioration for health monitoring purposes.
4. Larger bridges were selected for better and longer vibration response.
5. Bridges close to YSU campus were preferred for convenience, and to minimize time and cost of travel.

From a list of available single-span PSBB bridges in ODOT District 4, a set of six bridges, as shown in Table 2-1, was proposed, for data collection and modeling. Two bridges out of six proposed were finally selected for data collection. Another relatively newer bridge in Trumbull County was selected later to test the application software. The

MAH-45-0579 Bridge (MAH Bridge) is over West Branch of Mender Creek on the S. Salem-Warren/ Rt. 45 in Mahoning County, Ohio. It is a single-span, 84.5 ft long composite PSBB bridge built in July 1993. It consists of 48 in. wide and 42 in. deep 11 PSBBs under a 5.5 in. thick composite concrete deck. The ATB-322-1916 Bridge (ATB Bridge) is over Pymatuning Creek on Highway 322 in Ashtabula County, Ohio. It is an 85 ft long, single span PSBB bridge built in July 1988. It has nine 48 in. wide and 42 in. deep PSBBs with a 2.5 in. thick layer of asphalt concrete wearing surface. Figures 2-1 and 2-2 show pictures of the two selected bridges in Mahoning and Ashtabula Counties, respectively.

Table 2-1: List of bridges proposed to ODOT for data collection

Cty	Rte	SLM	Feature intersected	SFN	Future ADT	Date built	Total spans	Max span length	Overall structure length	Main structure type
ATB	322R	1916	Pymatuning creek	0406430	2,679	7/1/1988	1	84	85	231
ATB	193R	2019	Griggs creek	0405620	2,684	7/1/1991	1	60	64	231
ATB	006R	2469	Gravel Run	0400432	2,790	7/1/1991	1	60	61	231
MAH	045R	0579	W BR Meander creek	5001544	4,650	7/1/1993	1	85	88	231
MAH	534R	0925	Turkey Broth creek	5005809	4,525	7/1/1986	1	55	56	231
TRU	046R	2515	Mosquito creek	7802994	1,138	7/1/1985	1	75	76	231





A: Side view

B: Top view (Google Maps)

Figure 2-1: MAH Bridge.



A: Side view

B: Top view (Google Maps)

Figure 2-2: ATB Bridge.

## 2.2 SunSPOT Sensors and WSN

Sun Small Programmable Object Technology (SunSPOT) sensors are Java programmable embedded devices, which were used for the collection of real-time dynamic structural response of two bridges selected for this study. A basic SunSPOT

sensor contains accelerometer sensors, temperature and light sensors, radio transmitter, eight multicolored LEDs, 2 push-button control switches, 5 digital I/O pins, 6 analog inputs, 4 digital outputs, and a rechargeable battery (Oracle, 2012). A SunSPOT hardware kit shown in Fig. 2-3 includes two sensors, and a base station to communicate wirelessly with sensors. Figure 2-4 shows the internal parts of a base station and a SunSPOT sensor. Each SunSPOT sensor has a unique 16-digit media access control address and can capture acceleration vs. time data in all three axes simultaneously. In this research, only Z-axis (vertical axis) acceleration data were collected at 100 Hz frequency and 2g scale.



Figure 2-3: SunSPOT hardware kit.

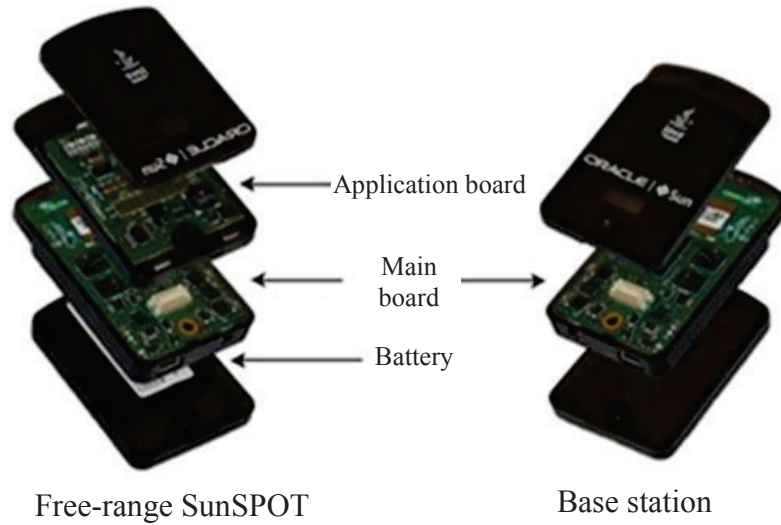


Figure 2-4: Internal parts of SunSPOT sensor and base station.

In order to prepare the SunSPOT sensors for data collection, two separate software packages were developed using Java. The first software was developed to control the functions of the base station to connect with the laptop, and to establish communication between SunSPOT sensors to collect data and to save them in Microsoft Excel format. The second software controls the functions of the accelerometer inside the free-range SunSPOT, the data collection sampling rate, and the data transmission to the base station. The SunSPOT sensors were tested and calibrated in a lab environment before deploying them in the field to collect the dynamic response of the selected bridges.

### 2.3 Moving Loads on Bridges

Vehicles needed for running the data collection tests were provided by the Mahoning and Ashtabula County Engineer’s Offices in coordination with ODOT and County personnel. Three standard two-axle dump trucks with different weights were used for the tests. These trucks include an Empty Truck, a Half-loaded Truck, and a Fully-

loaded Truck. The information about the trucks, their axle dimensions and weights, are shown in Appendix A as recorded by the Ohio State Highway Patrol. Figure 2-5 shows pictures of a two-axle truck while recording axle dimensions and weights.



A: Measuring truck axle dimensions

B: Measuring truck axle weights

Figure 2-5: Recording truck axle dimensions and weights.

## 2.4 WSN Setup and Data Collection

After the SunSPOT sensors were customized and prepared for field deployment, tests were run in coordination with ODOT and County personnel for data collection on the bridges.

### 2.4.1 WSN Setup

Two sets of wireless sensor networks were deployed simultaneously on the bridge during each truck run. Each set of the WSN included four SunSPOT sensors, one base station, and a laptop. SunSPOT sensors were numbered from 1 to 4 for base station 1 and 5 to 8 for base station 2. The base station and SunSPOT sensors were customized in such

a way that the sensors transmit data only to the assigned base station. In this way, the base station 1 in WSN 1 collects data only from sensors 1 to 4, while the base station 2 in WSN 2 collects the data only from sensors 5 to 8. Figure 2-6 shows the configuration of the two WSNs built with SunSPOT sensors, base stations and laptops. Each base station was connected to a laptop via a universal serial bus (USB) port to get the power and to send the collected data to the laptop. In order to ensure adequate power supply to the SunSPOT sensors, each of them was connected to an external battery throughout the entire test, as shown in Fig. 2-7.

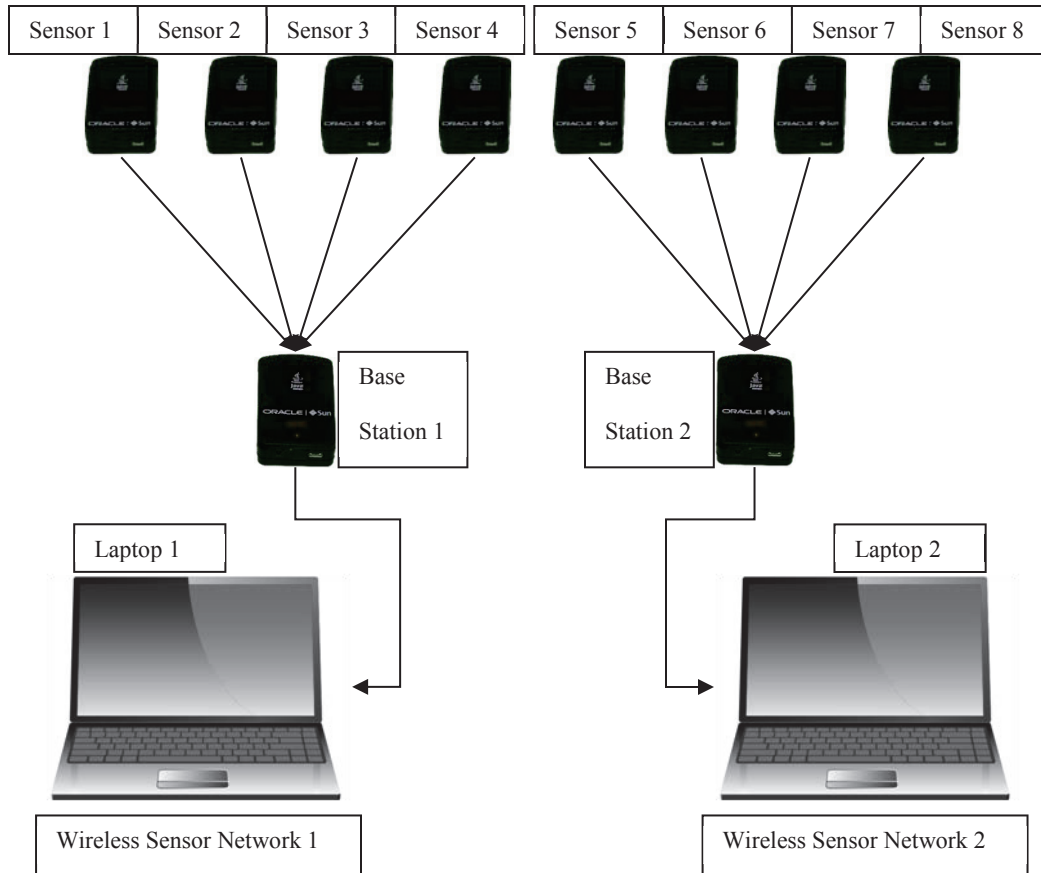


Figure 2-6: Configuration of two WSNs used on bridges.



Figure 2-7: SunSPOT sensors with external battery.

#### 2.4.2 Sensors and Truck Locations

Two sets of wireless sensor networks were attached on the bridge deck using the arrangement shown in Figs. 2-6 and 2-8. Since the maximum vibration is anticipated in the middle of the bridge, sensors were attached on the middle half of the bridge at 5 ft spacing, which also helped better communication between sensors and base stations. The truck path, as shown in Fig. 2.8, was delineated in a way that its centerline coincided with the longitudinal centerline of the bridge for even distribution of truck loads across the bridge.

During the first attempt in collecting the dynamic response of MAH Bridge with sensors attached on the bridge centerline, a test truck accidentally ran over and destroyed all eight sensors and the batteries. The data sets collected before the accident were incomplete and, therefore, were discarded. In order to avoid such damage to sensors during future data collections, sensor locations were shifted from the centerline to the side of the bridge, as shown in Fig. 2-8 for both MAH and ATB Bridges. Figure 2-9 shows pictures of data collection on both bridges.

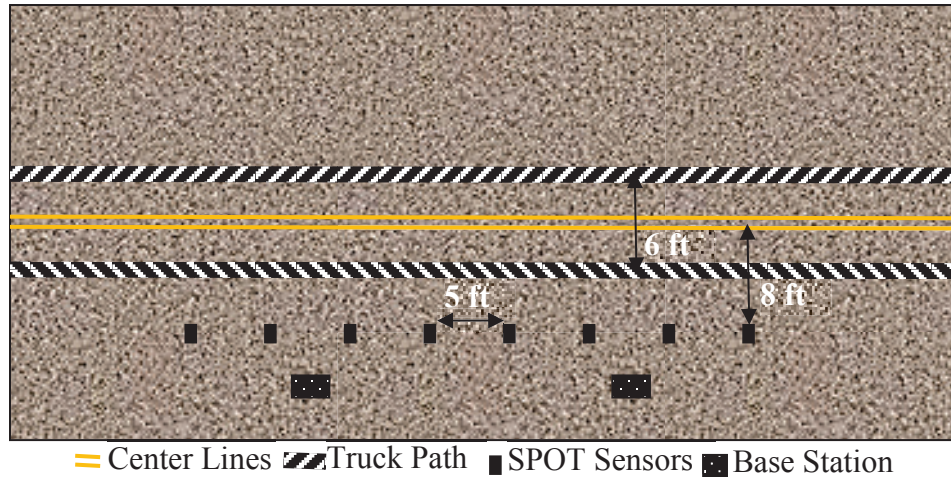


Figure 2-8: Graphical representation of truck path and sensor locations.



A: Data collection on MAH Bridge

B: Data collection on ATB Bridge

Figure 2-9: Field data collection.

### 2.4.3 Acceleration Data Collection

Before the test runs, ODOT and County personnel closed one lane of traffic on the bridge during taking measurements and installing sensors. Sensors locations were marked and cleaned before applying quick-setting glue to hold the sensor clips, which grip the sensors. The glue was also used to prevent unexpected vertical movement of the

sensors. In other words, the sensors were attached to be an integral part of the bridge. The same procedure was used prior to running the truck on MAH and ATB Bridges. Figure 2-9 also shows the attachment of sensors on MAH and ATB Bridge.

An Empty, a Half-loaded, and a Fully-loaded Truck were used for collecting bridge dynamic response. During the test runs, the truck drivers were instructed to drive over the centerline of the bridge and maintain a uniform speed. On the MAH Bridge, each truck ran three times at 10, 15, and 20 mph speed. Every single run produced 8 subsets of sensor data – one subset for each sensor. Since a total of 9 runs were performed on the bridge, a total of 72 subsets of acceleration data were collected on the bridge. While on the ATB Bridge, each truck ran four times at 10, 15, 20, and 25 mph speed. Therefore, a total of 96 subsets of acceleration data were collected on the bridge. The bridge acceleration versus time data for each run was recorded in real-time; sample of recorded data is shown in Appendix B. The accelerometer inside the SunSPOT sensors captured the analog bridge acceleration signals due to vibration under vehicular movement and converted them into electrical voltage. The voltage is then converted into a digital signal using the built-in analog-to-digital converter (ADC) in the sensor. All data collected from the sensors were time-stamped along with the 16-digit media access control address of respective sensor for easier identification and synchronization.

Due to near-freezing temperature during the data collection on the MAH Bridge, it is suspected that the glue might not set enough to prevent the vertical movement of sensors with respect to the bridge surface. Therefore, it might have absorbed part of the bridge vibration. Still the acceleration data on MAH Bridge were analyzed and found unacceptable for further use. In order to avoid such problems in future, a different type of



quick-setting epoxy, which sets in twenty minutes to prevent sensor movement, was used during the data collection on the ATB Bridge. Figure 2-10 shows ATB Bridge acceleration data under a Fully-loaded Truck at 25 mph speed.

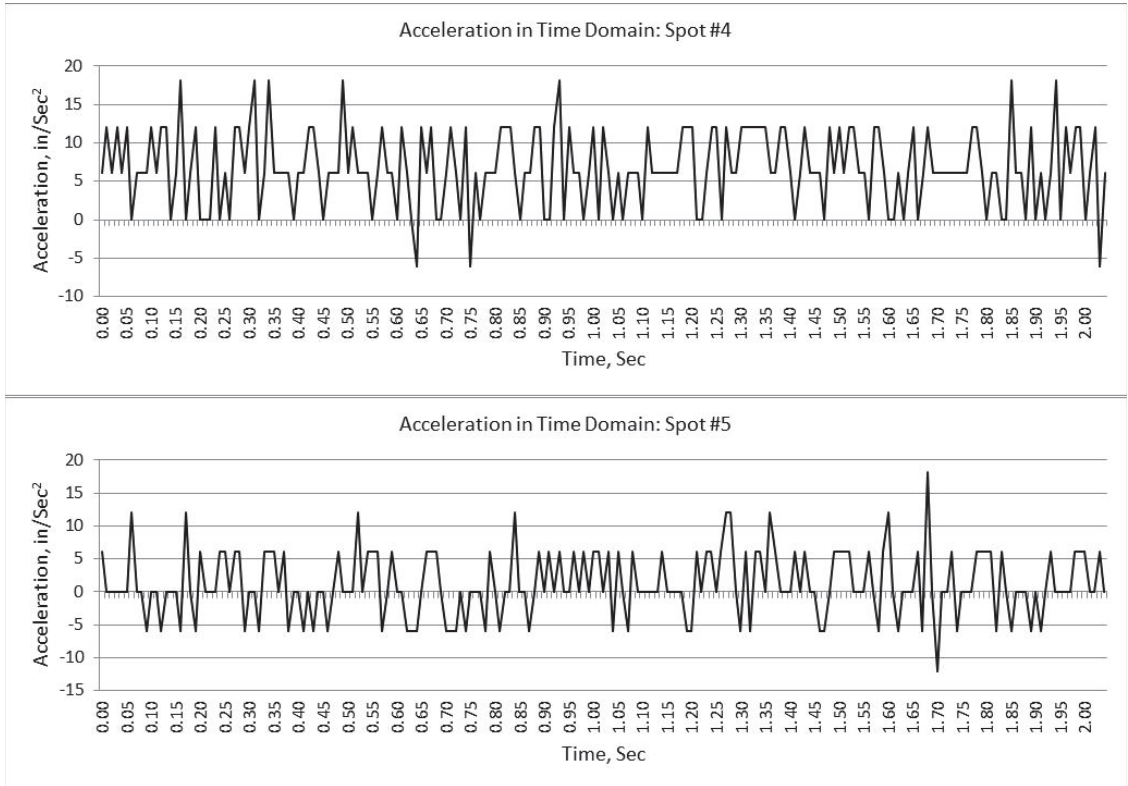


Figure 2-10: Acceleration of ATB Bridge in time domain.

## CHAPTER 3

### Modeling and Simulation

#### 3.1 Finite Element Modeling

The finite element method (FEM) is a numerical technique, which is used to find approximate solutions for boundary value problems in engineering, such as structural analysis, heat transfer, and fluid flow (Logan, 2001). In this research, ABAQUS/CAE 6.12-1 (SIMULIA, 2013) commercial finite element modeling and analysis software was used to create a full-scale three dimensional model of ATB Bridge at its newest condition (right after construction), and to find its dynamic response under vehicular loads. The geometric parameters and material properties, which were used to build the bridge model, were taken from the bridge plans that were provided by ODOT.

The development of a finite element (FE) bridge model using ABAQUS/ CAE includes modules, such as Part, Property, Assembly, Step, Interaction, Load, Mesh, and Job modules, from which ABAQUS/CAE generates an input file. After creating the model, it was simulated under moving vehicles with different speeds and weights mimicking the field data collection. The bridge model was submitted for analysis to record acceleration data at each sensor location mimicking the field configuration.

#### 3.2 Bridge Descriptions

The ATB Bridge is 85 ft long and 36 ft wide, and consists of nine 48 in. by 42 in. PSBBs, as shown in Fig. 3-1. The PSBBs were made with 5,500 psi concrete and ½ in. stress-relieved strands with ultimate strength of 270,000 psi. A 2½ in. thick asphalt

concrete wearing surface was also placed over the PSBBs. The PSBB layout plan and a typical cross-section of ATB Bridge are shown in Figs.3-2 and 3-3, respectively.

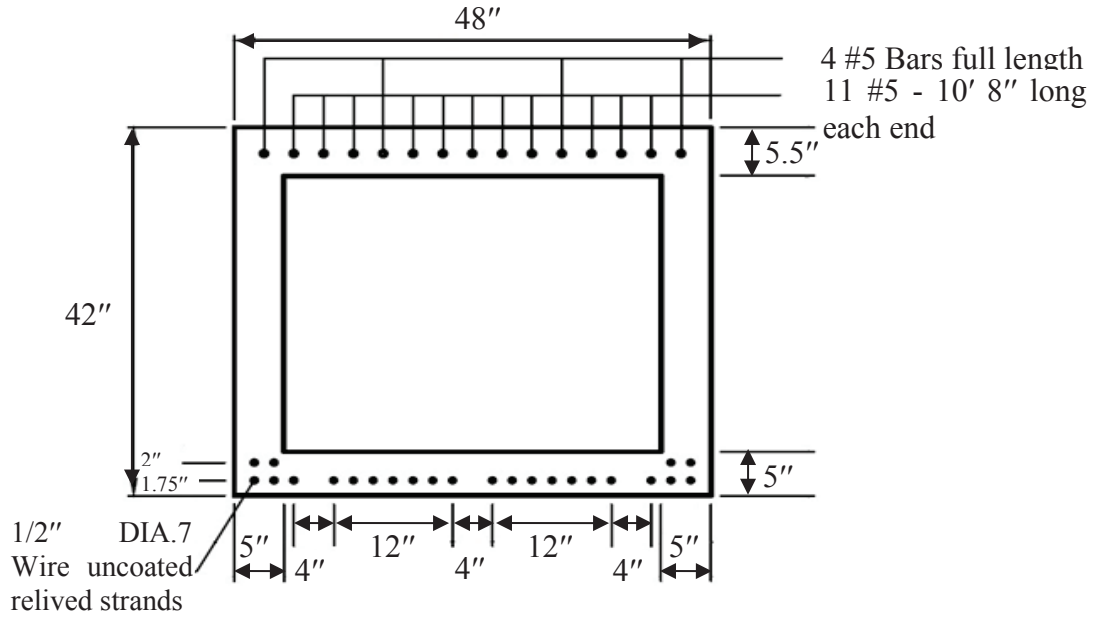


Figure 3-1: A typical PSBB cross-section of ATB Bridge.

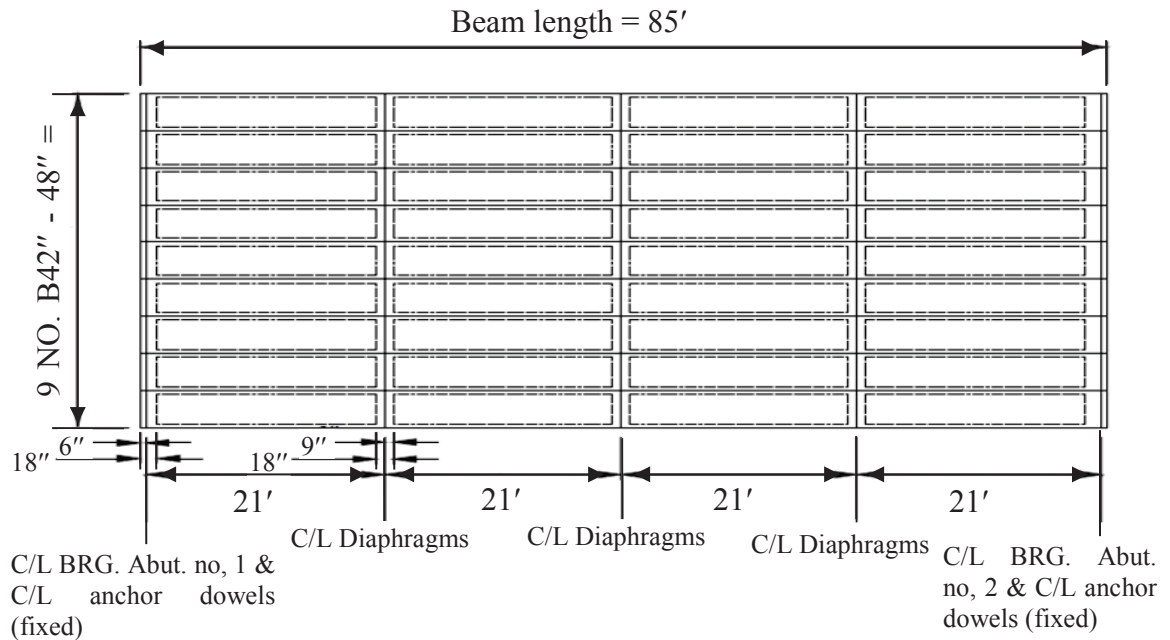


Figure 3-2: ATB Bridge PSBB layout plan.

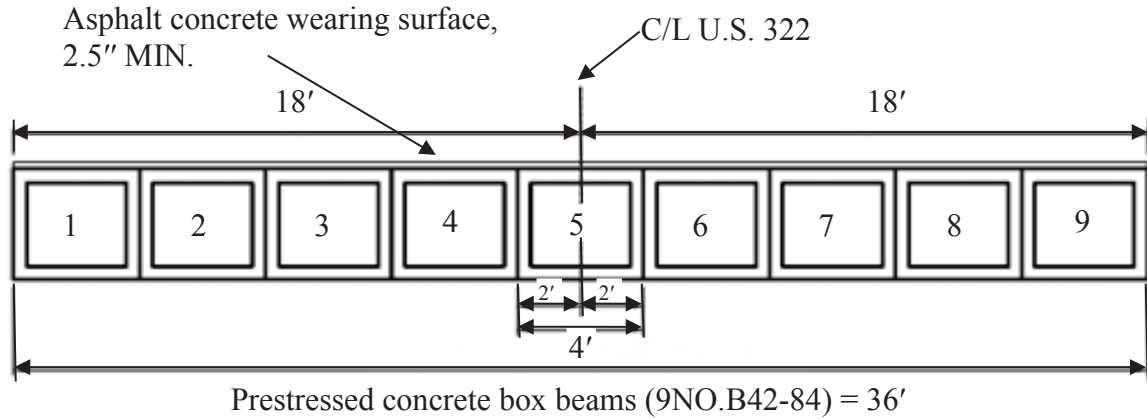


Figure 3-3: ATB Bridge cross-section.

### 3.3 FE Modeling of ATB Bridge

The FE modeling of ATB Bridge consists of various steps as described herein.

#### 3.3.1 Creating Model Parts

The part module was used to create and edit five different parts for the model using two features. Each one of these parts is located in its local coordinate system. Prestressed concrete box beam and asphalt concrete wearing surface parts were created using solid features, while reinforcing steel and prestressing strands parts were created using wire features. After creating the solid parts of the bridge model, multiple cut extrude and cell partition were used to create the ends of the beam, the internal diaphragms, the truck paths, and sensor locations. After creating the parts, the mesh module was used to control the element shape, meshing technique, element type, parts seeds, etc. The hexahedral element shape was used with structured meshing technique to generate the mesh. This technique applies pre-established mesh patterns for the model parts, which provide the most control over the mesh. For both PSBBs and the asphalt concrete wearing surface parts, the '3D Stress' eight-node linear brick elements were

used. The two-node linear ‘3D Truss’ elements were used for the reinforcing steel and the prestressing strands parts. Size of elements in the mesh was defined to be 10 in. This mesh size divided the bridge model into 50,772 elements. FE model parts are shown in Fig. 3-4.

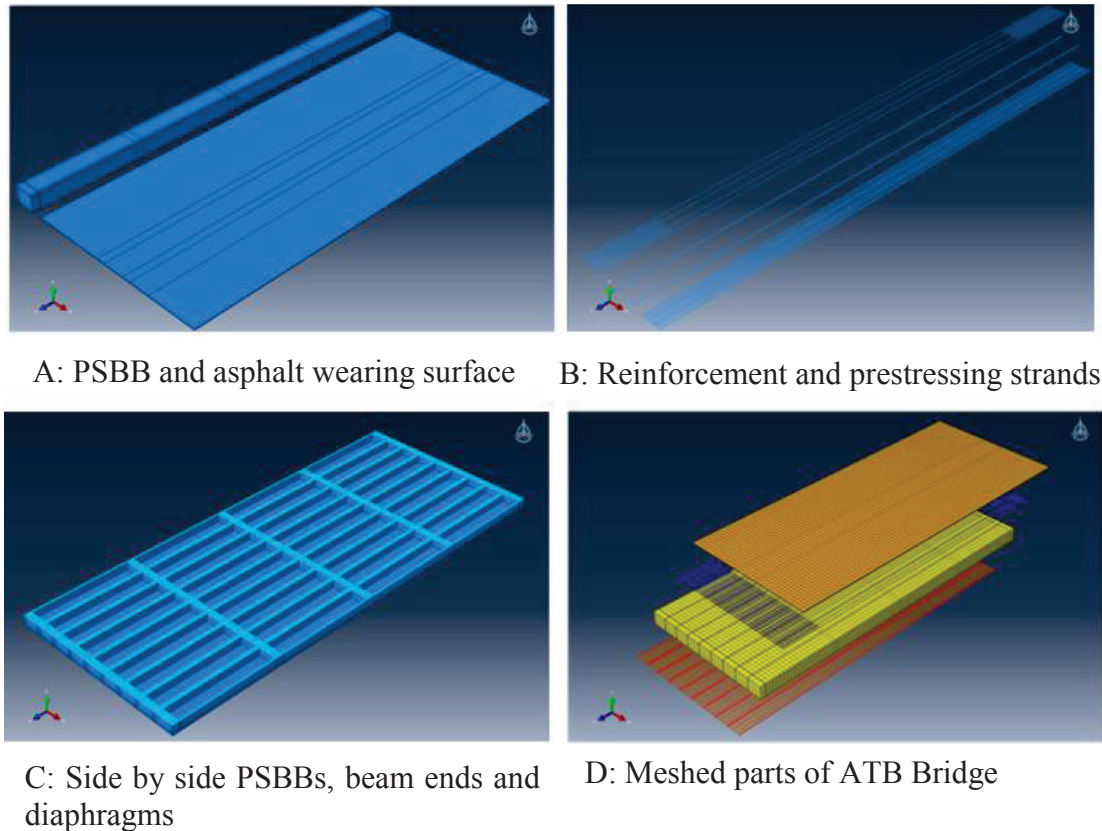


Figure 3-4: Parts of ATB Bridge model.

### 3.3.2 Defining Part Properties

The property module was used to define the material properties and the part sections. Four material properties were created to define prestressed concrete, asphalt concrete, steel reinforcement, and prestressing strands. Material property inputs in the FE model are shown in Table 3-1. The section editor was used to define the part sections. The section editor is divided into various categories and each category is divided into

different types. The solid category with homogenous type was used to define the PSBB and the asphalt concrete wearing surface. The beam category with truss type was used to define the reinforcing steel and the prestressing strands.

Table 3-1: Material properties of elements in ATB Bridge model

Part	Material	Properties		
		Density (lbf s <sup>2</sup> /in <sup>4</sup> )	Modulus of Elasticity (psi)	Poisson's Ratio
Prestressed concrete box beam	Prestressed concrete	2.246520589 E-4	4496060.776	0.15
Asphalt concrete wearing surface	Asphalt concrete	2.246520589 E-4	350000	0.35
Reinforcing steel	Steel	7.338633924 E-4	29000000	0.3
Prestressing strands	Steel	7.338633924 E-4	28500000	0.3

### 3.3.3 Creating Model Assembly

The assembly module was used to create part instances and to position the instances relative to each other in a global coordinate system. The part instances were positioned together by sequentially applying position constraints that align selected faces or edges, or by applying simple translations and rotations (SIMULIA, 2013). Figure 3-5(a) shows the different part instances that represent the bridge model assembly, while Fig. 3-5(b) shows the entire bridge model assembly after the reinforcing steel and the strands were embedded in the PSBBs. The assembly module was also used to create the contact surfaces between the part instances. These contact surfaces were used to define the interaction between the instances in the interaction module. In addition, the assembly module was used to define a set of the sensor node locations mimicking the field locations. A 10 in. mesh size was selected for the entire simulation.

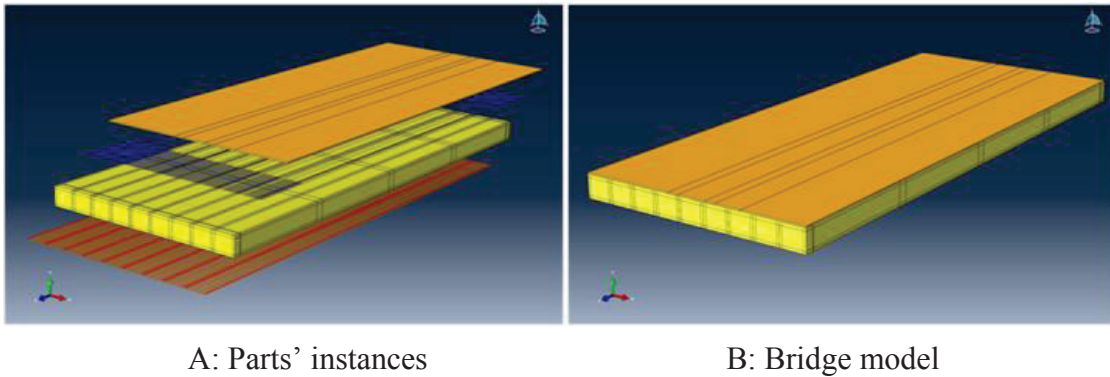


Figure 3-5: ATB Bridge: assembly model.

After creating the model assembly, the interaction module was used to define and manage the interaction and the constraints between the parts instances. The interaction properties section was used to define the concrete friction coefficient, which is equal to  $0.6\lambda$  with  $\lambda$  value equal to 1 for normal weight concrete, according to the American Concrete Institute (ACI) Building Code Section 11.6.4.3 (ACI, 2008). Contact surfaces were used as pairs to define the interaction surfaces between the PSBBs. No part was created for the transverse tie rod during the modeling, but the effect of the tie rods was taken into consideration by creating tie constraints at diaphragm locations between the PSBBs. Another tie constraint was created between the bottom of the asphalt concrete wearing surface and the top of the PSBBs. An embedded element technique was used to define the contact between the reinforcement or the prestressing strands and the PSBBs. This type of constraint is used to specify a group of embedded elements that lays in a group of host elements. The response of the host elements is used to constrain the translational degrees of freedom of the embedded elements (SIMULIA, 2013).

### 3.4 Load Generation

Loads, predefined fields, and boundary conditions were defined using the load module. Dead loads and truck loads were defined under the mechanical category. The dead load of the structure was defined using the gravity load (g). To define the truck load, VDLOAD user-subroutine was written using Fortran10.1.034. The VDLOAD user-subroutine is used to define the distributed load magnitude of the truck wheels as a function of position, time, and velocity. Twelve VDLOAD subroutines were created for different truck weights and speeds. For each one of these files, the speed of the truck was calculated in in./sec. and the weight of each wheel was assumed to be uniformly distributed over the contact area. The contact area was taken as a single rectangular area of 20 in. width and 10 in. length according to AASHTO Section 3.6.1.2.5 (AASHTO, 2007). Moreover, axle spacing, truck width, and truck paths were taken into consideration during the development of VDLOAD subroutines. The effect of prestress was included in the models by applying stress in the prestressing strands. The stress was applied under the mechanical category in the predefined section. The value of stress was calculated by dividing the final tension force of 21,700 lb per strand (adopted from ODOT plans) after all losses (ODOT, 1972) by the area of a prestressing strand. The fixed type of anchor dowels was used at the beams ends. Therefore, fixed boundary conditions were assumed during the simulations and were applied at the bottom of the beams ends, as shown in Fig. 3-6.



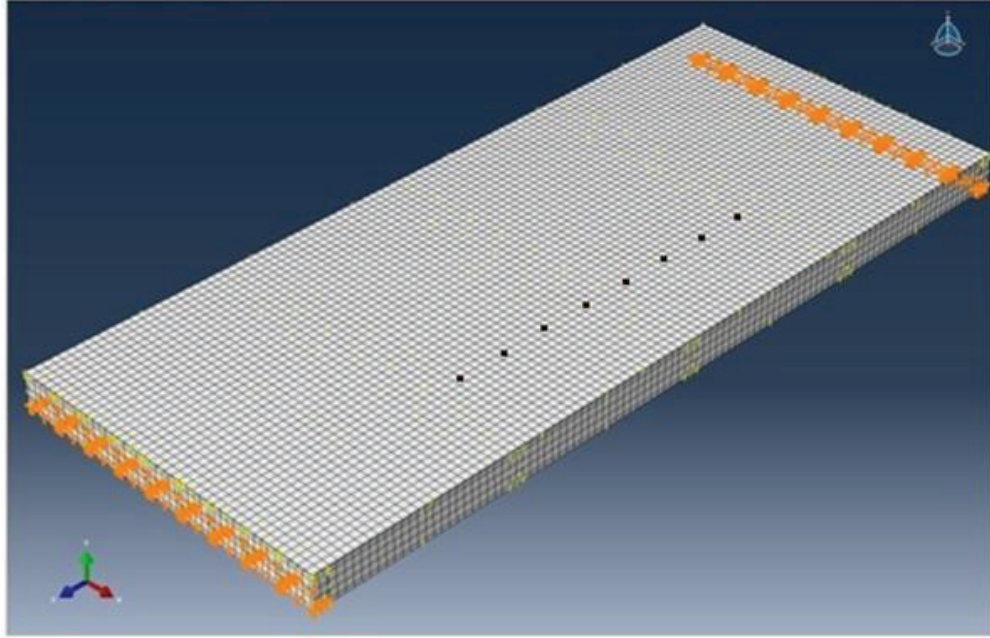


Figure 3-6: ATB Bridge model: sensor locations and boundary conditions.

### **3.5 Bridge Model Analysis**

The bridge model analysis includes static and dynamic analyses and frequency analysis as described herein.

#### **3.5.1 Static and Dynamic Analyses**

After developing the three-dimensional FE model of the ATB Bridge, the input file was submitted to ABAQUS/Standard and ABAQUS/Explicit using the job module to perform analysis and generate an output database. The analysis of the model was performed in two stages using two types of simulation procedure: Static-general and dynamic-explicit. The first stage of analysis was performed using ABAQUS/Standard to analyze the effect of the prestress, as shown in Fig. 3-7. ABAQUS/Standard is a general-purpose analysis product that can solve a wide range of linear and nonlinear problems

involving static, dynamic, and thermal problems, when accurate stress solutions are of main interest (SIMULIA, 2013).

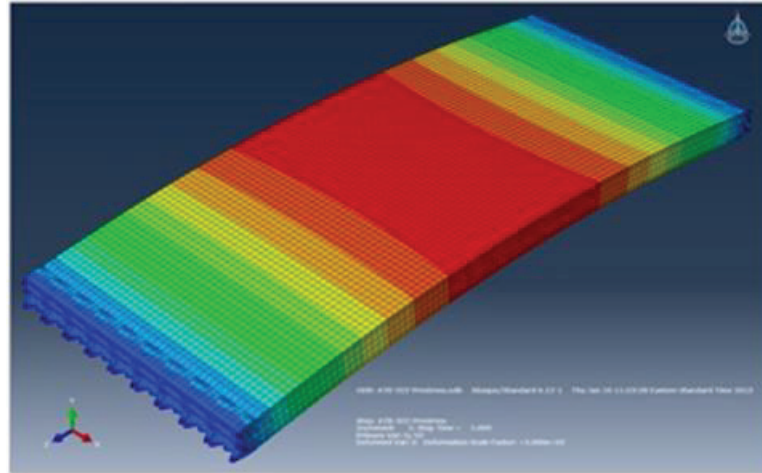


Figure 3-7: Prestress effect on ATB Bridge model (exaggerated).

The second stage of analysis was performed using ABAQUS/ Explicit to find the bridge dynamic response under vehicular loads. ABAQUS/Explicit is a special-purpose analysis product that uses an explicit dynamic finite element formulation. It is a suitable and very efficient tool that provides accurate solutions for high-speed, large, and non-linear dynamics simulations (SIMULIA, 2013). During the real-time data collection, trucks passed the bridge at four different speeds, and the sensors collected acceleration data at 100 Hz. Therefore, the analysis time period, the maximum time increment in the dynamic-explicit analysis procedure, and the data output request were modified during the simulation to mimic the conditions during the real-time data collection. Time needed for the trucks to pass the bridge at each speed was calculated and taken into consideration to determine the analysis time period for the bridge modeling. In addition, time increment and data output request were changed to 0.01 second to mimic the real-time data

collection rate. Before the second stage of analysis, the effect of the prestress from the first stage of analysis was imported to the dynamic model using the initial state type of load under the predefined field section. The analysis was performed 12 times on the ATB Bridge model with 12 different Fortran VDLOAD user-subroutines. At the end of each analysis, the acceleration data in Y-direction (vertical) at the sensor node locations were requested for output. Finally, the requested output was saved as Microsoft Excel files. Figure 3-8 shows the dynamic response of the ATB Bridge model under the Fully-loaded Truck at 25 mph. In addition to the acceleration data, the displacement of the bridge model under the vehicular loads were also requested for output and saved as Microsoft Excel files. Sample of acceleration and displacement data is shown in Appendix B. The analysis data were later used to analyze the ATB Bridge model behavior.

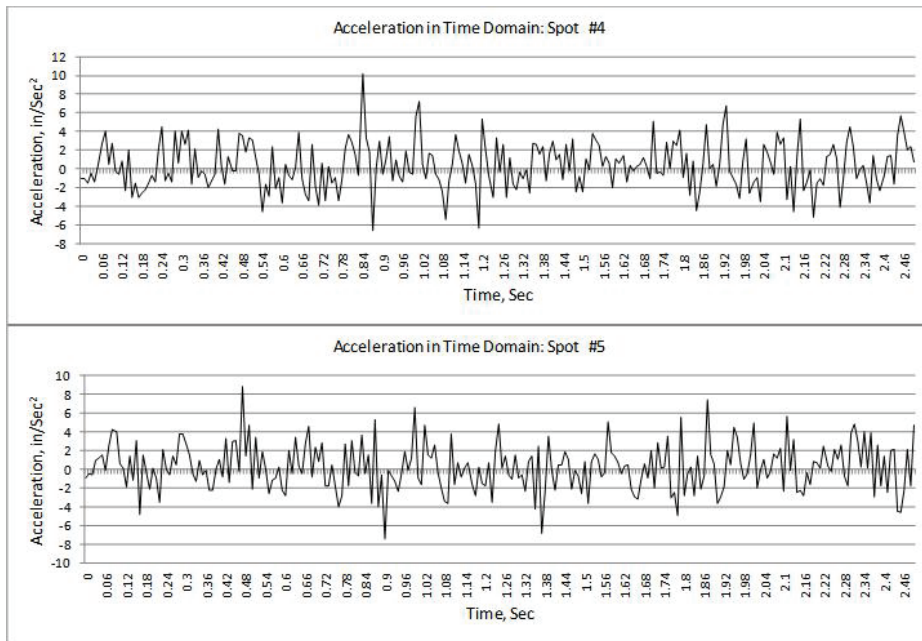
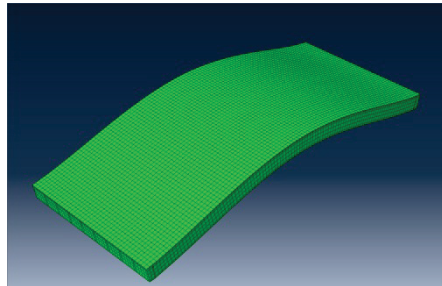


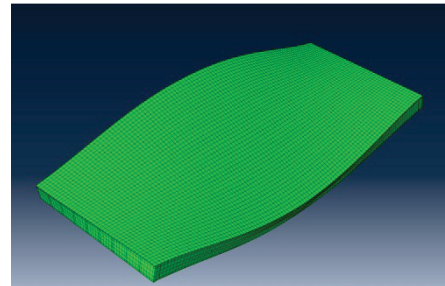
Figure 3-8: Acceleration of ATB Bridge model in time domain.

### 3.5.2 Frequency Analysis

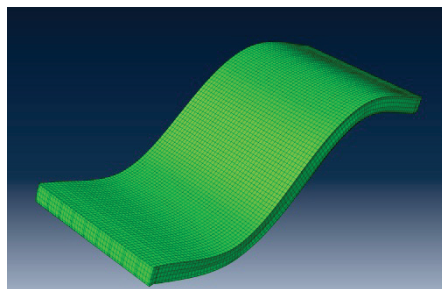
Frequency analysis procedure was used to find the mode shapes and the corresponding vibration frequencies of the ATB Bridge model. In order to prepare the model for analysis, the same procedure was used incorporating necessary changes in the step and load modules. In the step module, frequency type of analysis step was created. No load was defined in the load module. The analysis result of the frequency model is shown in Fig. 3-9, which shows the first four vibration mode shapes of the ATB Bridge model.



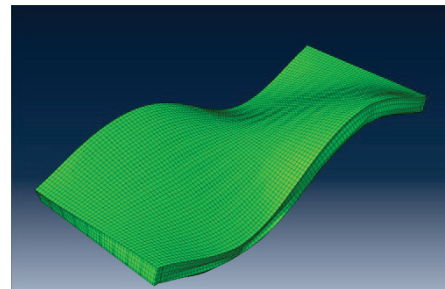
A: Mode 1 – Frequency = 5.41 Hz



B: Mode 2 – Frequency = 10.41 Hz



C: Mode 3 – Frequency = 14.5 Hz



D: Mode 4 – Frequency = 22 Hz

Figure 3-9: Vibration mode shapes of ATB Bridge model.

### 3.6 FE Model Validation

The most challenging task in finite element modeling and analysis is to validate a finite element model assumed to represent a real structure. In this study, the results of static and frequency analyses were compared to hand calculations and bridge dynamic characteristics, which were obtained by analyzing the field data, to validate the FE model of ATB Bridge.

The static analysis of the ATB Bridge model at its newest condition included application of a static pressure of 10 psi on a 12 in. wide strip across the bridge width, as shown in Fig. 3-10. The pressure was applied at the middle of the span to uniformly distribute its effect across the bridge. A static analysis was performed, and the results for the maximum stress and the highest mid-span deflection were obtained. The total mass of the ATB Bridge model was also obtained from the analysis output. The results of this analysis were compared to the results of approximate hand calculations, as shown in Table 3-2, in order to validate the ATB Bridge model.

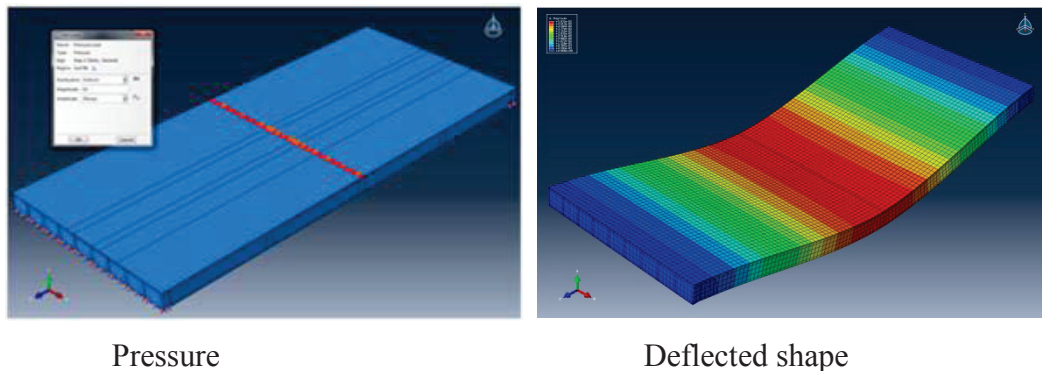


Figure 3-10: ATB Bridge model validation: static analysis.

Table 3-2: Comparisons of FE model and hand calculations

Items	FEA	Hand calculations
Maximum stress	73 psi	78.14 psi
Maximum deflection	0.05 in.	0.036 in.
Total mass	2193.1 lb.s <sup>2</sup> /in	2154.32 lb.s <sup>2</sup> /in
Vibration frequency	3.5505 Hz	3.4383 Hz *

\*Bridge frequency from field data.

On the day of data collection on the ATB Bridge, no noticeable section loss was detected by visual inspection of the bridge. Therefore, the decrease in structural stiffness of the bridge appears to be due to the material deterioration. The modulus of elasticity (MOE) of the PSBB is the primary material property of the bridge in the FE modeling. Therefore, the MOE of the PSBB in current condition was calculated and used to create another FE model using the same procedure to represent the ATB Bridge at its current condition. After creating the model, frequency analysis procedure was used to find the fundamental vibration frequency of the bridge in its current condition, as shown in Fig 3-11. The first modal frequency of the model was compared to the frequency of the bridge, which was determined from the analysis of the real-time acceleration data (data analysis discussed in more details in Chapter 4), as shown in Table 3-2.

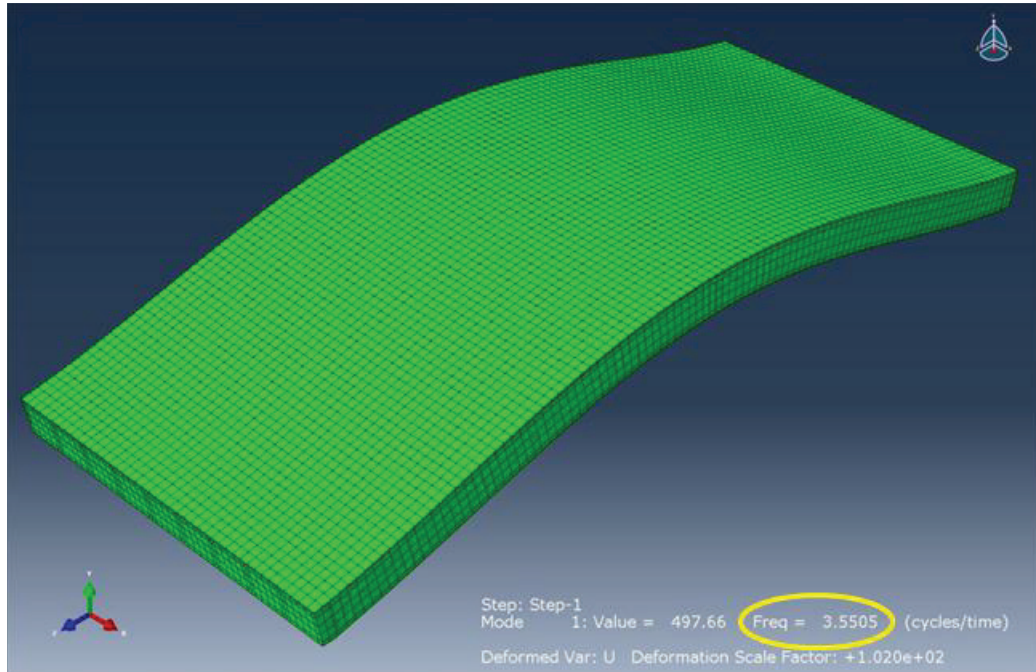


Figure 3-11: ATB Bridge model validation: frequency analysis.

It can be seen from Table 3-2 that the results from the ATB Bridge model and hand calculations are fairly close. In view of the above analyses and comparisons, it can be concluded that the ATB Bridge model very closely represents the real structure at its newest condition. The hand calculations in details are shown in Appendix C.

## CHAPTER 4

### Bridge Load Rating

#### 4.1 Equation of Motion and Natural Frequency

Degrees of freedom (DOF) can be defined as the number of independent coordinates, which are needed to describe the configuration of a structure at any instant of time. In reality, structures have an infinite number of DOF. Therefore, an infinite number of independent coordinates are needed to determine the configuration of a structure (Tedesco, 1999). However, if a structure is idealized as a single degree of freedom (SDOF) spring-mass system, as shown in Fig. 4-1, then the equation of motion can be expressed by Eq. 4.1.

$$m\ddot{X} + c\dot{X} + kX = F(t) \quad (4.1)$$

Where,  $\ddot{X}$  is the acceleration of the system,  $\dot{X}$  is the velocity of the system,  $X$  is the displacement of the system,  $m$  is the system mass,  $c$  is the system damping coefficient,  $k$  is the system stiffness, and  $F(t)$  is the time-dependent force that acts on the system and causes the forced vibrations.

After some simple calculations, the natural circular frequency,  $\omega$ , of the system can be expressed by Eq. 4.2. At the same time, it can be expressed in term of the natural frequency,  $f$ , of the system by Eq. 4.3. Therefore, the natural frequency of the system can be expressed by Eq. 4.4.



$$\omega = \sqrt{\frac{k}{m}} \quad (4.2)$$

$$\omega = 2 \pi f \quad (4.3)$$

$$f = \frac{1}{2 \pi} \sqrt{\frac{k}{m}} \quad (4.4)$$

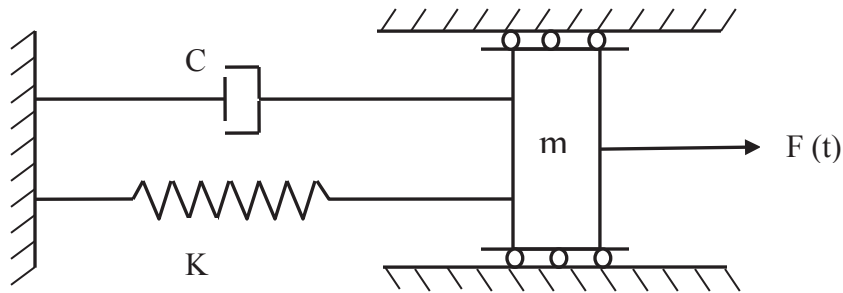


Figure 4-1: SDOF spring- mass system.

Assuming that a bridge behaves like a SDOF spring-mass system, the stiffness of the spring (herein bridge) can be calculated by Eq. 4.5, if the fundamental vibration frequency and the mass of the system are known. The calculated system stiffness can be used to estimate the load bearing capacity of a bridge.

$$k = 4 \pi^2 f^2 m \quad (4.5)$$

## 4.2 Bridge Response Analysis

The peak amplitude and fundamental frequency of a bridge under forced vibration are two important parameters for estimating the load bearing capacity of a bridge. The bridge dynamic response under forced vibration was captured as acceleration in the time domain. The acceleration of the existing bridge in the field and the ATB Bridge model was transformed into frequency domain by performing Fast Fourier Transform (FFT) (Cooley and Tuckey, 1965). The peak-picking algorithm was used to pick the peak amplitudes and their corresponding frequencies from the FFT data of the bridge in the field and the ATB Bridge model.

The acceleration data in the frequency domain may have multiple peaks, which represent various modes of movement, but the most dominant peak will represent the most critical mode. The FFT data shows the dynamic response of ATB Bridge has clear dominant peaks for all 8 sensors. Figure 4-2 shows the dynamic response of the bridge in the frequency domain due to vibration caused by the Fully-loaded Truck at 25 mph. Using the peak-picking algorithm, the peak amplitudes and their corresponding frequencies for the field bridge were recorded and shown in Tables 4-1 and 4-2. The FFT data from the dynamic response of the ATB Bridge model under truck loads also show clear dominant peaks. The peak amplitudes and their corresponding frequencies of the ATB Bridge model (bridge in its newest condition) are shown in Tables 4-3 and 4-4. Figure 4-3 shows the dynamic response of the ATB Bridge model due to the Fully-loaded Truck at 25 mph speed.

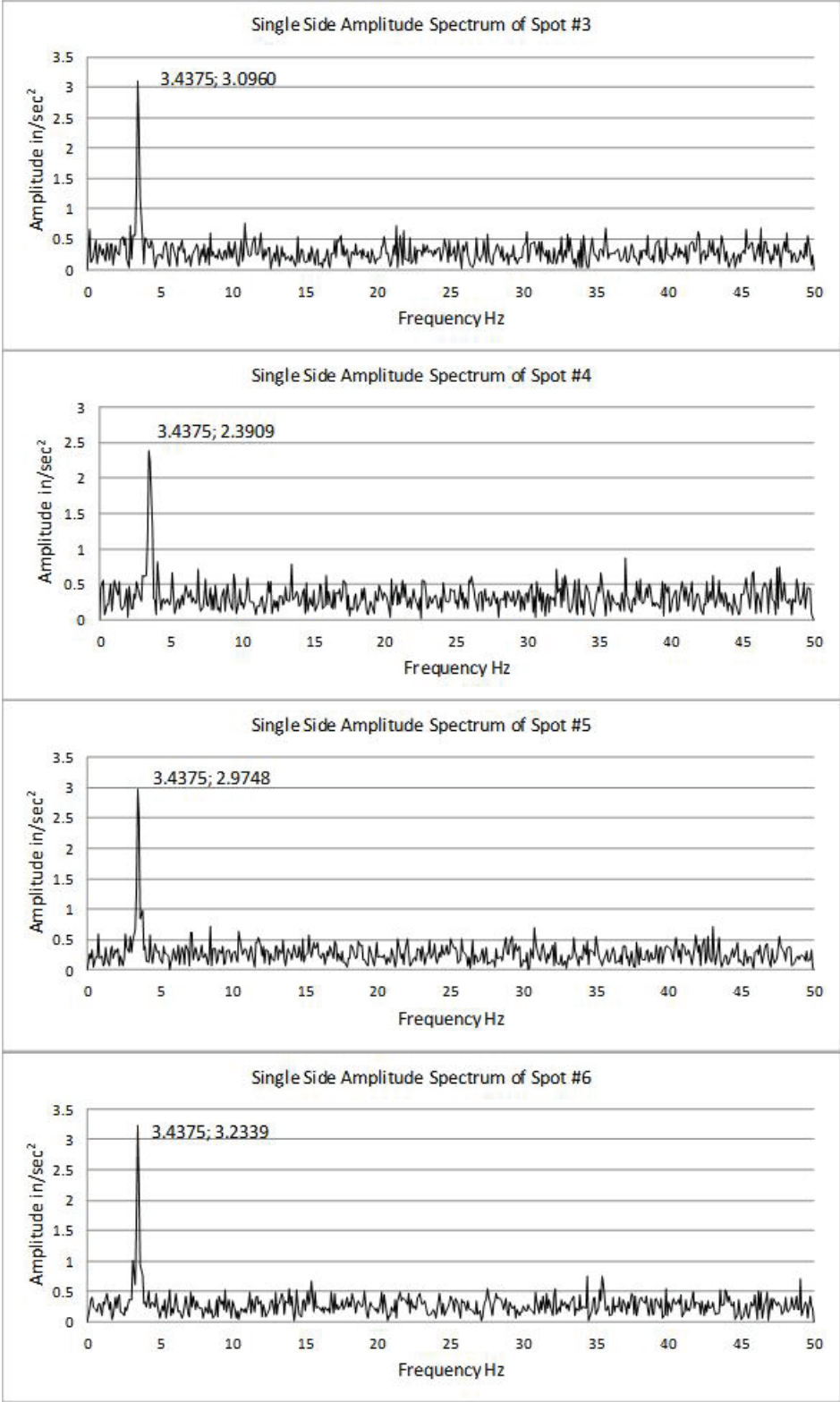


Figure 4-2: Amplitude vs. frequency data of ATB Bridge.

Table 4-1: ATB Bridge peak amplitude

Real-Time Data Collection: Peak Acceleration Amplitude (in/sec <sup>2</sup> )									
Truck	Speed (mph)	Sensors							
		1	2	3	4	5	6	7	8
Empty Truck	10	0.7955	0.597	0.7658	0.8394	0.6801	0.7456	0.7105	0.4776
	15	0.7943	0.8453	0.9635	0.8881	0.9248	0.9499	0.8416	1.0852
	20	0.8432	0.7587	0.7021	0.7884	0.6611	0.7167	0.6472	1.0723
	25	0.8073	0.8019	0.7125	0.8151	0.8608	0.6567	0.5814	0.813
Half-loaded Truck	10	0.8845	0.8044	0.9869	0.9961	1.3109	0.9244	0.7336	0.691
	15	1.0971	1.2088	1.4901	1.6912	1.7886	1.1231	1.4277	1.2162
	20	1.1092	1.3114	2.4062	1.6515	1.6394	1.7315	1.6019	1.5444
	25	0.8173	0.9448	0.7717	0.8007	0.9907	0.7483	1.0102	0.8908
Fully-loaded Truck	10	0.8461	0.6119	0.7755	0.8548	0.7183	0.7742	0.7592	0.5558
	15	1.1393	1.4843	1.3318	1.5946	1.3892	1.4673	1.4981	1.4568
	20	0.8217	1.0709	1.228	1.0229	1.2248	1.2033	1.188	0.8998
	25	2.5957	2.7362	3.096	2.3909	2.9748	3.2339	2.6264	1.927

Table 4-2: ATB Bridge frequency at most dominant peak

Real-Time Data Collection: Bridge Frequency (Hz)									
Truck	Speed (mph)	Sensors							
		1	2	3	4	5	6	7	8
Empty Truck	10	3.4375	3.3333	3.4375	3.9583	3.5417	3.5417	3.5417	2.8125
	15	3.6458	3.75	3.5417	3.5417	3.6458	3.6458	4.0625	3.5417
	20	2.6639	3.4836	3.5861	2.5615	3.0738	3.1762	2.6639	3.1762
	25	3.5861	2.6639	2.8689	3.5861	2.0492	2.6639	2.5615	2.6639
Half-loaded Truck	10	3.3333	2.6042	3.4375	3.4375	3.4375	3.4375	3.4375	3.4375
	15	3.4836	3.5861	3.5861	3.5861	3.5861	3.6885	3.5861	3.5861
	20	3.4375	3.4375	3.4375	3.4375	3.4375	3.4375	3.4375	3.4375
	25	3.2292	3.2292	3.75	3.125	3.2292	3.2292	3.4375	3.3333
Fully-loaded Truck	10	3.4375	2.8125	3.6458	3.4375	2.7083	3.125	3.4375	3.6458
	15	3.4836	3.4836	3.4836	3.4836	3.4836	3.4836	3.4836	3.4836
	20	3.4375	3.4375	3.2292	3.3333	2.9167	3.3333	3.125	3.4375
	25	3.4375	3.4375	3.4375	3.4375	3.4375	3.4375	3.4375	3.4375

Table 4-3: ATB Bridge model peak amplitude

ATB Bridge Model: Peak Acceleration Amplitude (in./sec <sup>2</sup> )									
Truck	Speed (mph)	Sensors							
		1	2	3	4	5	6	7	8
Empty Truck	10	0.5294	0.2984	0.4945	0.5077	0.5687	0.4296	0.2183	0.3795
	15	0.3576	0.4166	0.4659	0.4674	0.4497	0.2944	0.3791	0.3963
	20	0.7109	0.577	0.7819	0.7988	0.7202	0.6839	0.5583	0.418
	25	0.5873	0.5714	0.5218	0.7581	0.7141	0.5787	0.3943	0.3928
Half-loaded Truck	10	0.4098	0.3394	0.4379	0.4731	0.4216	0.4165	0.3513	0.3316
	15	0.3333	0.4069	0.412	0.4331	0.465	0.4983	0.4891	0.4372
	20	0.6223	0.5463	0.6973	0.4903	0.6712	0.4677	0.4859	0.6263
	25	0.5233	0.5311	0.5102	0.6342	0.6508	0.5634	0.5165	0.5053
Fully-loaded Truck	10	0.4286	0.3219	0.5194	0.3818	0.4271	0.364	0.4584	0.3795
	15	0.4564	0.3835	0.3632	0.4527	0.4199	0.4588	0.4282	0.549
	20	0.7109	0.577	0.7819	0.7988	0.7202	0.6839	0.5583	0.418
	25	0.6551	0.7739	0.714	0.595	0.7333	0.6172	0.6364	0.622

Table 4-4: ATB Bridge model frequency at most dominant peak

ATB Bridge Model: Bridge Frequency (Hz)									
Truck	Speed (mph)	Sensors							
		1	2	3	4	5	6	7	8
Empty Truck	10	5.3946	5.3946	5.3946	5.3946	5.3946	5.3946	4.995	5.5944
	15	5.3683	5.4931	5.3683	5.4931	5.3683	5.3683	5.3683	5.4931
	20	5.4446	5.4446	5.4446	5.4446	5.4446	5.4446	5.4446	5.4446
	25	5.3892	5.3892	5.3892	5.3892	5.3892	5.3892	5.5888	5.3892
Half-loaded Truck	10	5.3946	5.3946	5.3946	5.3946	5.3946	5.3946	5.3946	5.3946
	15	5.4931	5.4931	5.4931	5.4931	5.3683	5.4931	5.3683	5.4931
	20	5.4446	5.4446	5.4446	5.4446	5.4446	5.4446	5.4446	5.4446
	25	5.3892	5.3892	5.3892	5.3892	5.3892	5.3892	5.3892	5.3892
Fully-loaded Truck	10	5.3946	5.3946	5.3946	5.4945	5.3946	5.3946	5.3946	5.5944
	15	5.4931	5.3683	5.2434	5.3683	5.3683	5.4931	5.4931	5.4931
	20	5.4446	5.4446	5.4446	5.4446	5.4446	5.4446	5.4446	5.4446
	25	5.3892	5.3892	5.3892	5.3892	5.3892	5.3892	5.3892	5.3892

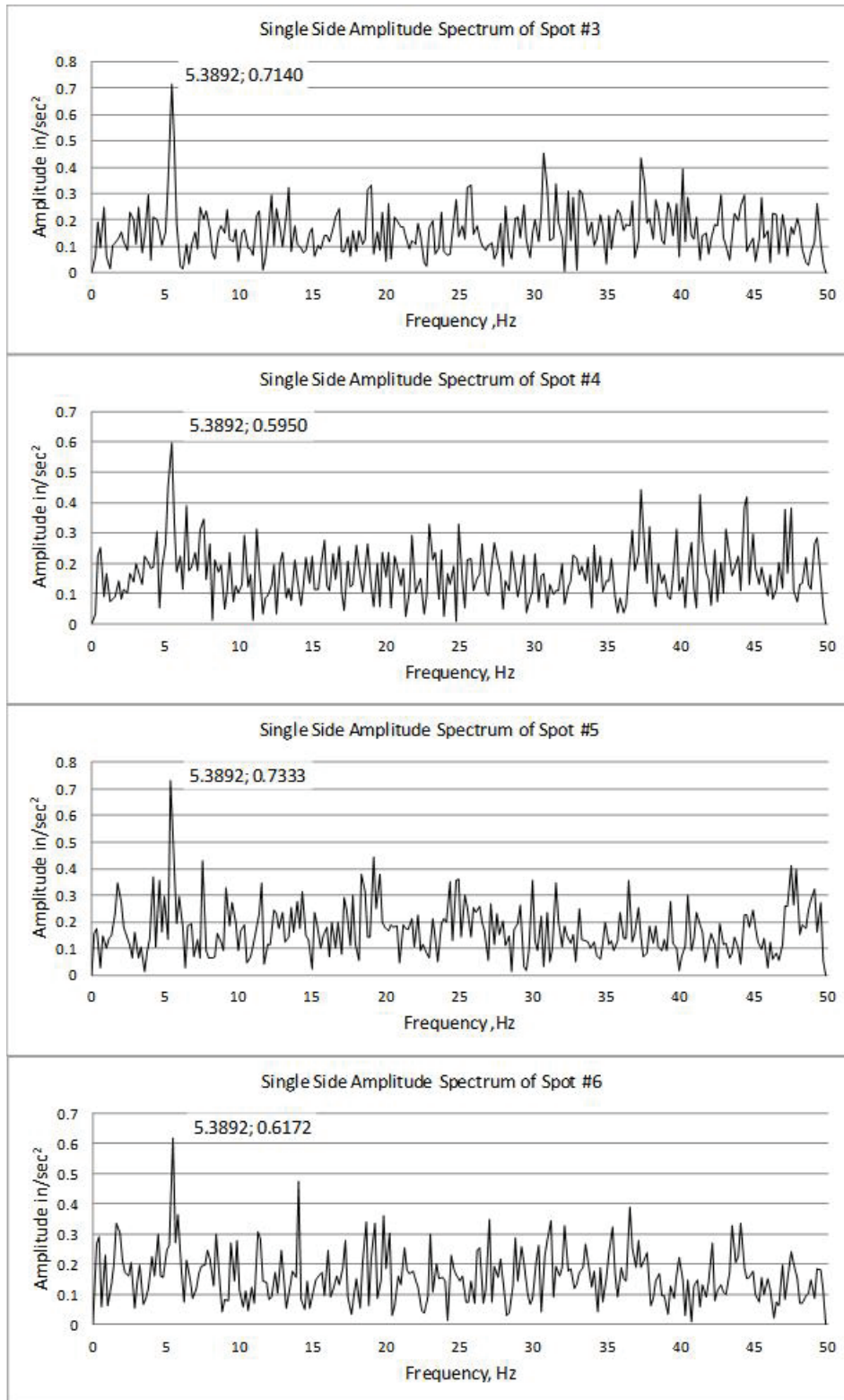


Figure 4-3: Amplitude vs. frequency data of ATB Bridge model.

### **4.3 Load Rating Methodology**

In order to estimate the load rating of a bridge, its stiffness in current condition should be calculated. For calculating the stiffness of ATB Bridge, it was assumed to be a single beam with distributed mass and stiffness, and fixed end support conditions. A structure with these assumptions will exhibit an infinite number of degrees of freedom due to its flexural deformation. However, if a structure is idealized as a SDOF system by assuming that the structure vibrates only in one predetermined vibration pattern (Tedesco, 1999), then the equation of motion can be expressed by Eq. 4.1, and the stiffness of the bridge can be calculated by Eq. 4.4 provided the fundamental vibration frequency and the mass of the system are known. The system stiffness can be used accordingly to estimate the load bearing capacity of a bridge. Systems idealized with these assumptions are known as generalized single degree of freedom system.

#### **4.3.1 ATB Bridge Fundamental Frequency**

The fundamental (or the first bending) frequency of a bridge is needed prior to calculating its bending stiffness. It was assumed that the frequency at the most dominant peak amplitude for each sensor is the fundamental frequency. This is a reasonable assumption for a single span bridge (Chen, 2002). To verify this assumption, the displacement data of the ATB Bridge model under different truck runs were collected and saved as Microsoft Excel files. The displacement data in the time domain were transformed into the frequency domain by using FFT. The most dominant amplitude peaks in the frequency domain were recorded, as shown in Table 4-5, to verify the vibration mode shape by plotting amplitude with sensor locations, as shown in Fig. 4-4.

As expected, the vibration mode of the ATB Bridge model under the vehicular loads was the first bending mode shape with frequency equal to 5.4688 Hz.

Table 4-5: ATB Bridge model: FFT results for displacement data

ATB Bridge Model / Fully-loaded Truck at 25 mph.			
Sensors	Bridge frequency (Hz)	Displacement Amplitude (in)	Sensors location on the bridge
1	5.4688	0.167696493	25
2	5.4688	0.197527442	30
3	5.4688	0.218794456	35
4	5.4688	0.229578996	40
5	5.4688	0.229578288	45
6	5.4688	0.218794332	50
7	5.4688	0.197524574	55
8	5.4688	0.16769027	60

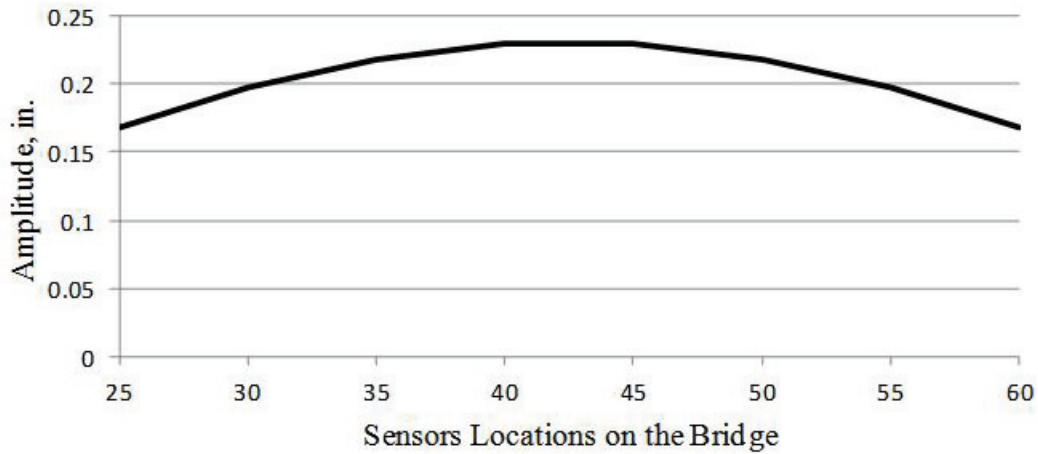


Figure 4-4: ATB Bridge model: mode shape under vehicular loads.

In addition, the frequency analysis results of the ATB Bridge model show that the first vibration mode of the bridge is a bending mode at 3.5505 Hz and 5.416 Hz in its current and newest condition, respectively. Comparing these results with the frequencies of ATB Bridge in the field (Table 4-2) and the ATB Bridge model (Table 4-4) verify the



assumption that the frequency of ATB Bridge under vehicular loads is the first bending frequency.

### 4.3.2 Idealized Bridge and Load Rating Equations

In order to idealize the ATB Bridge as a single beam with fixed end support conditions in a generalized SDOF system, as shown in Fig. 4-5, it is necessary to assume a displacement configuration or shape function,  $\varphi(x)$ , for the beam that satisfies its kinematic and natural boundary conditions. Once the fundamental frequency of the beam is known, the effective stiffness,  $K_e$ , and the effective mass,  $M_e$ , can be calculated after deriving the shape function of the vibration pattern. The shape function of a fixed-fixed beam can be expressed by Eq. 4.6.



Figure 4-5: Beam with fixed end supports.

$$\varphi(x) = y_0 \left(\frac{x}{L}\right)^2 \left(1 - \frac{x}{L}\right)^2 \quad (4.6)$$

Where,  $y_0$  is the vibration coefficient, and  $L$  is the PSBB beam length. By using the shape function, the effective mass and effective stiffness were calculated using Eqs. 4.7 and 4.8, and 4.9 and 4.10, respectively.

$$M_e = \int_0^L m \{\varphi(x)\}^2 dx \quad (4.7)$$

$$M_e = \frac{y_0^2 m_t}{630} \quad (4.8)$$

$$K_e = \int_0^L EI \{\varphi''(x)\}^2 dx \quad (4.9)$$

$$K_e = \frac{4 EI y_0^2}{5 L^3} \quad (4.10)$$

Where,  $m_t$  is the total mass of the bridge (lb\*S<sup>2</sup>/in), and EI is the effective flexural rigidity of the bridge (lb\*in<sup>2</sup>). Using the natural frequency expressed by Eq. 4.11, and the effective mass and stiffness of the system, it can be seen that the only unknown term is the effective flexural rigidity, EI<sub>Effective</sub>. Therefore, the EI<sub>Effective</sub> of the system can be calculated using Eqs. 4.12 and 4.13.

$$f = \frac{1}{2\pi} \sqrt{\frac{K_e}{M_e}} \quad (4.11)$$

$$f = \frac{1}{2\pi} \sqrt{\frac{\frac{4 EI y_0^2}{5 L^3}}{\frac{y_0^2 m_t}{630}}} \quad (4.12)$$

$$EI_{\text{Effective}} = \frac{f^2 * \pi^2 * L^3 * m_t}{126} \quad (4.13)$$

The maximum deflection,  $\Delta$ , at the middle of the beam can be expressed by Eq. 4.14. Using the load displacement relationship in Eq. 4.15, and the calculated EI<sub>Effective</sub> of the system, bridge stiffness can be calculated using Eq. 4.16.

$$\Delta = \frac{PL^3}{192 EI} \quad (4.14)$$

$$K = \frac{P}{\Delta} \quad (4.15)$$

$$K = \frac{192 * EI_{\text{Effective}}}{L^3} \quad (4.16)$$

Where, P is the bridge capacity. According to AASHTO Section 2.5.2.6.2 (AASHTO, 2007), the maximum allowable deflection for bridges with and without sidewalks are L/1000 and L/800, respectively. Using the maximum allowable deflection of the bridge and its calculated stiffness, the maximum allowable load capacity of the bridge can be estimated by Eq. 4.17.

$$P = K * \Delta \quad (4.17)$$

In order to eliminate the dynamic effect of a moving truck to achieve the static load capacity of a bridge, the dynamic load allowance or the dynamic load factor of acceleration (DLFA) should be used. The value of the dynamic load allowance that is used in design is equal to 1.33, as suggested in AASHTO Table 3.6.2.1-1 (AASHTO, 2007). On the other hand, the DLFA, which is the dynamic interaction between a moving vehicle and a bridge, can be obtained by using the accelerometer data. The DLFA is the ratio of the acceleration amplitude of a bridge under a vehicle at high speed (15 to 60 mph) to the acceleration amplitude of the bridge under a vehicle at low speed, as shown in Eq. 4.18. Therefore, the static bridge capacity after incorporating the dynamic effect can be expressed by Eq. 4.19.

$$DLFA = \frac{\text{acceleration amplitude for a vehicle at high speed}}{\text{acceleration amplitude for a vehicle at low speed}} \geq 1.33 \quad (4.18)$$

$$\text{Bridge Capacity} = \frac{P}{DLFA} \quad (4.19)$$

These equations are necessary for estimating the load rating of a single span bridge with fixed end support conditions. The derivation of the load rating equations for other ends support conditions are shown in Appendix D.

#### 4.4 Load Rating of ATB Bridge

Following the stated equations in Section 4.3, load rating of ATB Bridge was calculated for the three trucks (Empty, Half-loaded, and Fully-loaded) as shown in Table 4-6. By knowing the frequencies at the maximum peak amplitudes of ATB Bridge under the vehicular loads, the bridge span length and its total mass, the effective flexural rigidity of the bridge was calculated using Eq. 4.13. Using the load displacement relationship and the calculated  $EI_{\text{Effective}}$ , the bending stiffness of the bridge in the current condition was calculated by using Eq. 4.16. The bending stiffness of the bridge was used later to estimate the load bearing capacity for each sensor during each truck run using Eq. 4.19. The average of the load rating for the 8 sensors for each run was calculated later. Finally, to estimate the load rating of the bridge for each truck, the truck speed weighted average capacity was calculated as shown in Table 4-6. The bending stiffness,  $EI_{\text{Effective}}$ , and DLFA tables are shown in Appendix B.

Table 4-6: ATB Bridge load rating for different trucks

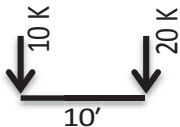
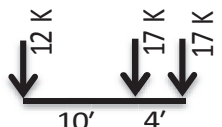
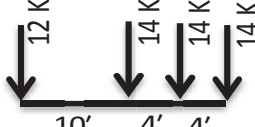
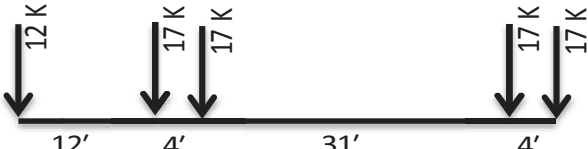
Truck weight (Ton)	Speed (mph)	Bridge capacity (Ton)		
		Average capacity for the 8 sensors	Truck speeds weighted average capacity	Rating factor
9.75	10	185.986	157.797	16.184
	15	207.878		
	20	144.358		
	25	127.224		
13.55	10	132.412	139.119	10.267
	15	154.072		
	20	141.923		
	25	130.587		
16.15	10	64.481	66.977	4.147
	15	70.680		
	20	63.142		
	25	68.822		

The load rating summary of ATB Bridge provided by ODOT is shown in Table 4-7. BARS software was used to perform the load rating of the bridge in 1993. VIRTIS is the new software developed and recommended by AASHTO (AASHTO, 2013) for load rating of highway bridges. Load rating results from BARS and VIRTIS seem very close. The load rating of a bridge using BARS and VIRTIS is expressed as a rating factor or in terms of tonnage for a particular vehicle. Vehicle weights and load configurations are shown in Table 4-8, which was taken from ODOT Bridge Design Manual, Section 900: Bridge Load Rating (ODOT BDM, 2004).

Table 4-7: Load rating of ATB Bridge using BARS and VIRTIS

VIRTIS Software			BARS Software		
Live load	Load rating (ton)	Rating factor	Live load	Load rating (ton)	Rating factor
OH-2F1	70.63	4.708	OH-2F1	73	4.867
OH-3F1	72.03	3.132	OH-3F1	74.4	3.234
OH-4F1	74.18	2.747	OH-4F1	76.7	2.84
OH-5C1	110.45	2.761	OH-5C1	110.5	2.762

Table 4-8: Ohio legal load vehicles weight and load configuration.

OHIO LEGAL LOADS		
Load designation	Load configuration	Gross vehicle weight
2F1		15 Tons
3F1		23 Tons
4F1		27 Tons
5C1		40 Tons

#### 4.5 Load Rating Flow Chart

This research was aimed at developing a method and application software for load rating of PSBB bridges based on their dynamic response. The geometric inputs for the application software are based on bridge element dimensions shown in Fig. 4-6. Figures

4-7 to 4-9 show the input page and flow charts of the load rating method, which were used to develop the load rating application software. This tool can be quickly deployed in the field to estimate the load bearing capacity of a PSBB bridge by collecting its dynamic response under trucks with known weights and speeds. The load rating output of the application software will be in terms of a rating factor (RF) or tonnage for a particular vehicle. In order to find the load rating of a bridge, a particular vehicle needs to be run at two different speeds.

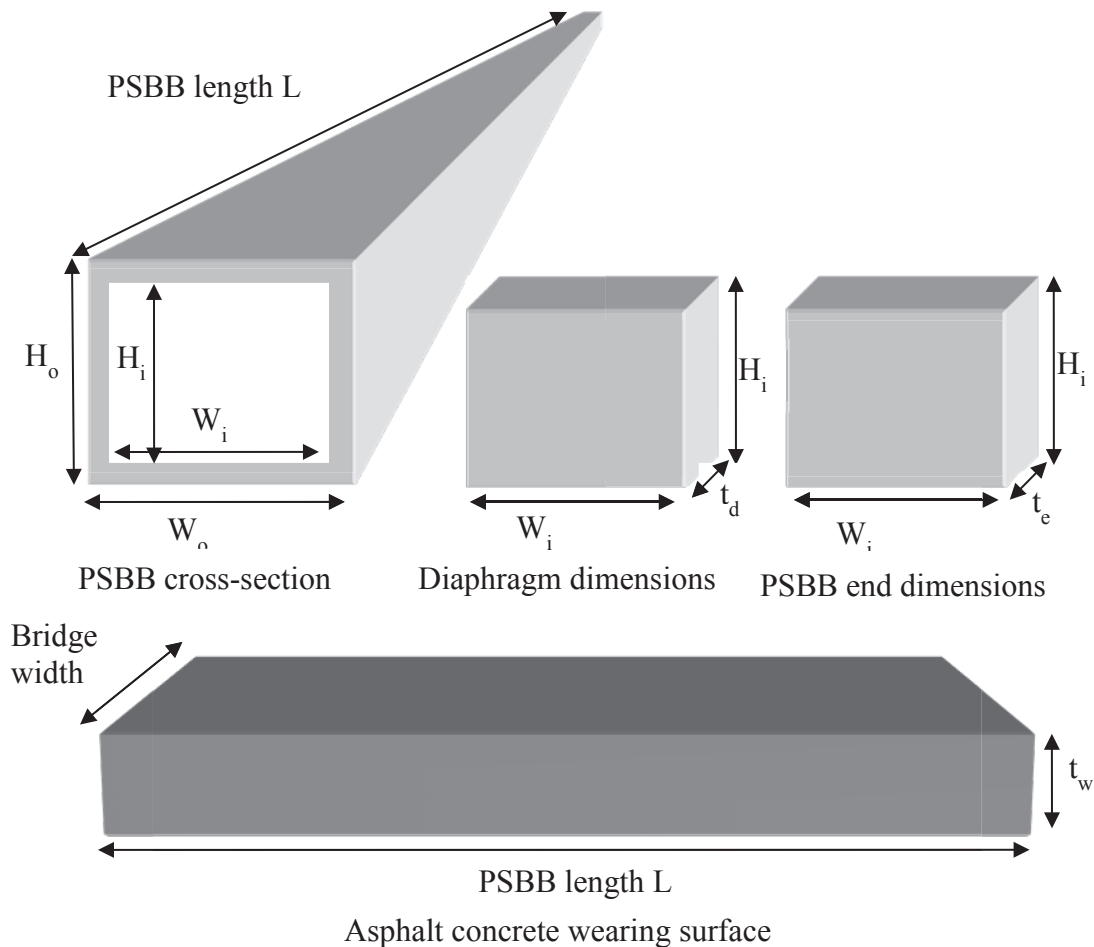


Figure 4-6: Bridge geometric properties.

Inputs:

1. L : Box Beam (PSBB) Length  (in)
2.  $W_o$  : Box Beam Outside Width  (in)
3.  $W_i$  : Box Beam Inside Width  (in)
4.  $H_o$  : Box Beam Outside Height  (in)
5.  $H_i$  : Box Beam Inside Height  (in)
6.  $n_b$  : Number of Box Beams
7.  $n_d$  : Number of Diaphragms per Box Beam
8.  $t_d$  : Thickness of Diaphragms  (in)
9.  $t_e$  : Thickness of Box Beam ends  (in)
10.  $t_w$  : Thickness of Asphalt Concrete Wearing Surface  (in)
11.  $f'_c$  : 28-day Compressive Strength of Concrete  (psi)
12.  $w_c$  : Unit Weight of Concrete  (lb/ft<sup>3</sup>)
13. Determine if the bridge with pedestrian sidewalks. (Drop Down menu)
  - a) No (the allowable deflection  $d = L/800$ )
  - b) Yes (the allowable deflection  $d = L/1000$ )
14. Bridge End Supports. (Drop Down menu)
  - a) Fixed-Fixed
  - b) Fixed-Hinged
  - c) Simply Supported
15. Truck Weight
  - a) T1 =  (lb)
  - b) T2 =  (lb)
  - c) T3 =  (lb)
16. Truck Speed
  - a) V1 (low) =  (mph)
  - b) V2 (high) =  (mph)

Figure 4-7: Load rating input page.



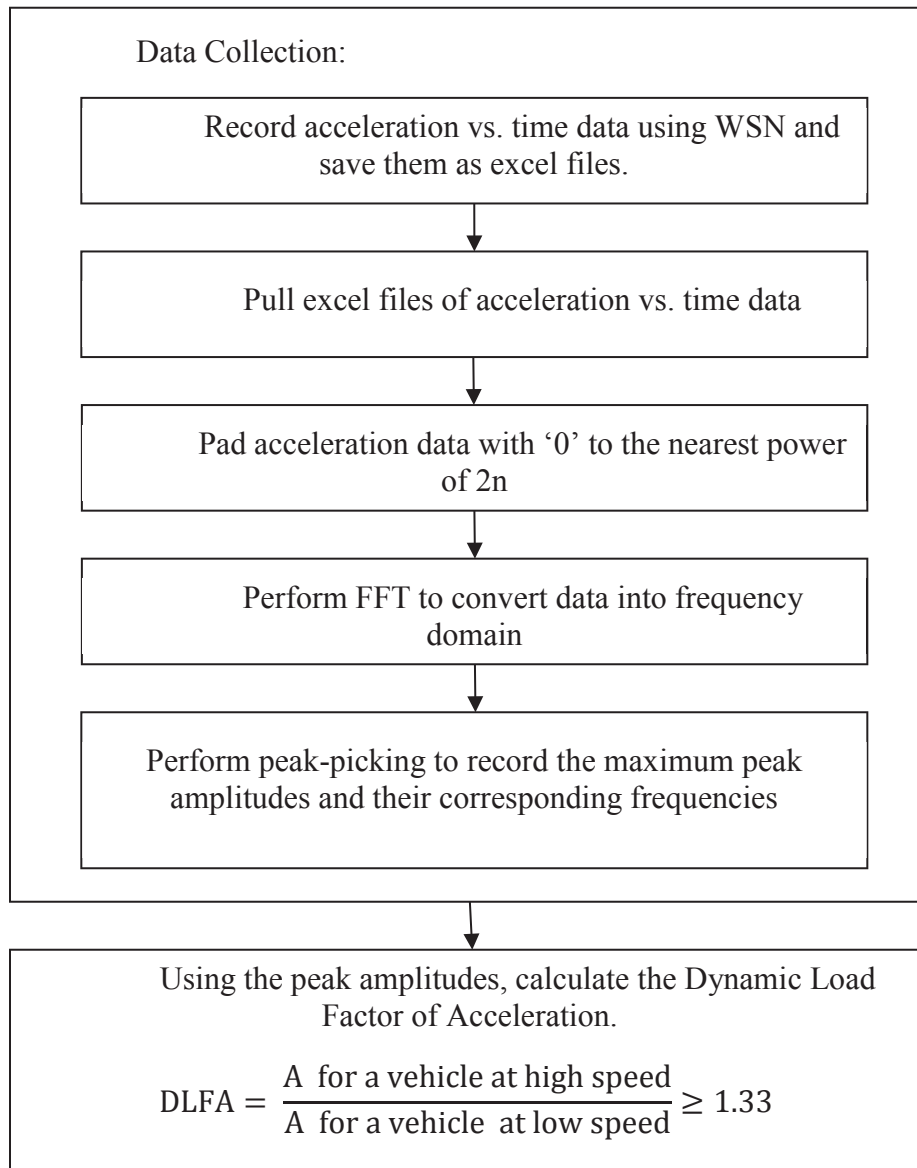


Figure 4-8: Load rating flow chart.

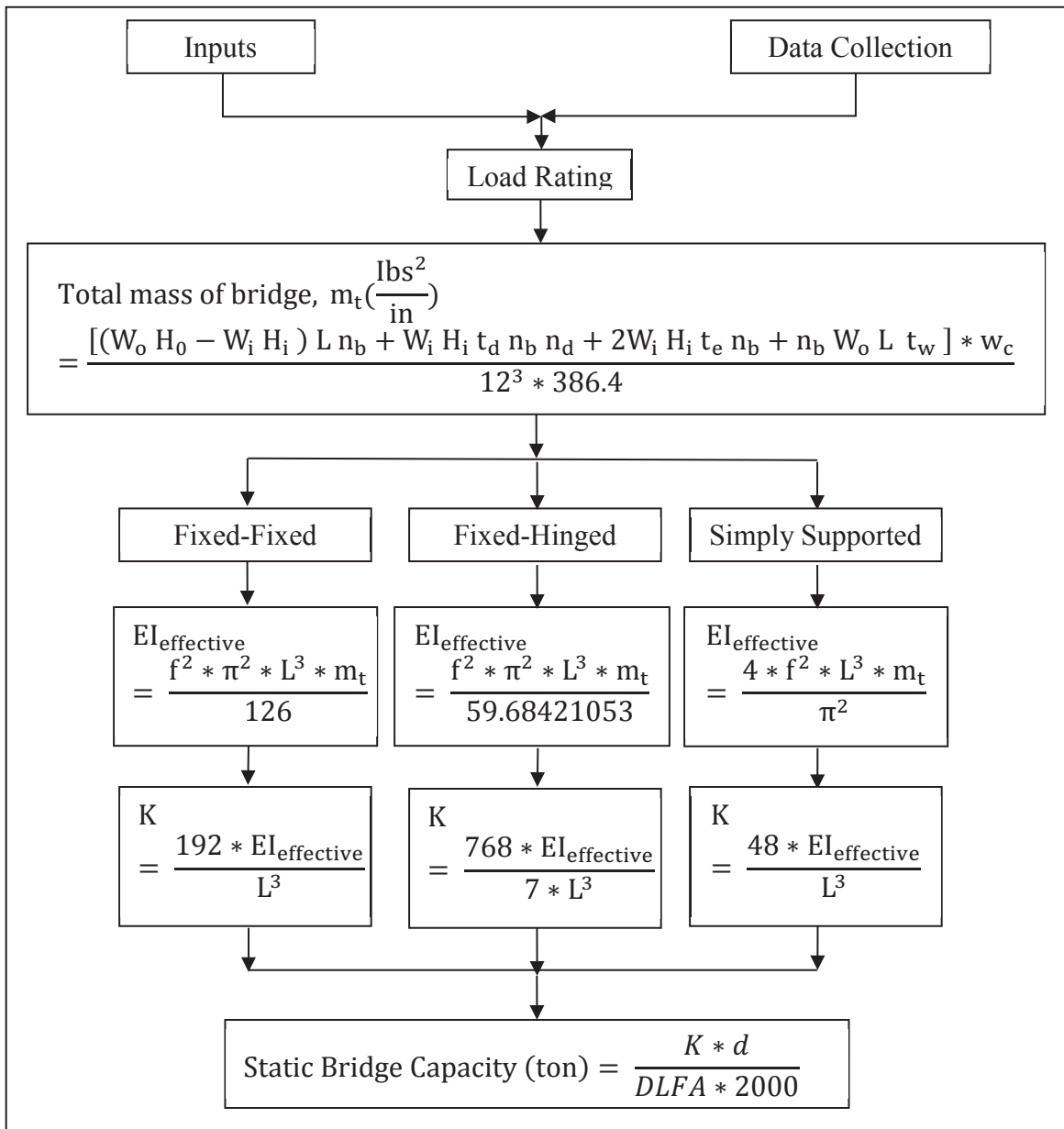


Figure 4-9: Load rating flow chart (continued).

## 4.6 Application Software and Validation

Microsoft's .NET4.5 framework was used to develop the application software based on the flow chart and the research outcomes of ATB Bridge. The application software "ODOTApp" includes two tabs "Input Parameters" and "Bridge Assessment," as shown in Figs. 4-10 and 4-11, respectively. The Inputs Parameters tab of the application software includes bridge geometric parameters, materials properties, support conditions, truck weight and dynamic response of a bridge under a heavily loaded truck at two different speeds. These parameters are self-explanatory, and they are available from the bridge design and construction plans.

The screenshot shows the 'Input Parameters' tab of the 'Bridge Condition Assessment and Load Rating' application. The window title is 'Bridge Condition Assessment and Load Rating'. The interface is divided into several sections:

- Box Beam:** PSBB Length (in.), Outside Width (in.), Inside Width (in.), Outside Height (in.), Inside Height (in.), Number of Box Beams, Number of Diaphragms / Box Beam, Diaphragm Thickness (in.), Box Beam End Thickness (in.).
- Concrete:** 28-day Compressive Strength (psi), Unit Weight (pcf).
- Bridge:** Pedestrian sidewalks (radio buttons for Yes and No, with No selected), End Supports (dropdown menu showing Fixed-Fixed), Wearing Surface Thickness (in.).
- Truck:** Truck #1, Weight (lb), Speed #1 (mph), Speed #2 (mph).

A 'Load Sensor Data' button is located at the bottom right, and a red message 'Sensor Data Not Loaded!' is displayed below it.

Figure 4-10: Input Parameters tab of ODOTApp application software.

The Bridge Assessment output tab includes two buttons: Start Analysis and View Report buttons, and two output boxes: Bridge Load Rating and Bridge Condition Rating. The analysis can be started by clicking the Start Analysis button. Once the analysis is complete, the analysis report can be viewed by clicking the View Report button. The report will contain the tables and results of the analysis. The summary of the analysis results is shown in two output boxes, the left box displays the bridge load rating based on the truck weight and the right box displays the bridge condition rating based on a scale of 0-9.

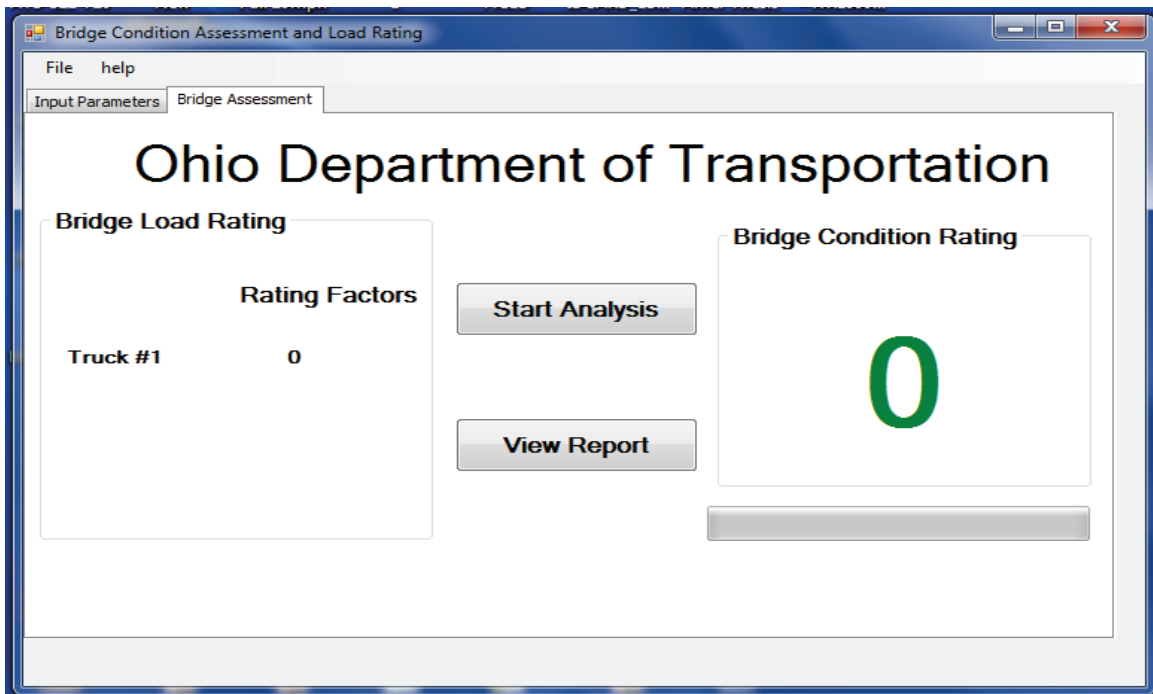


Figure 4-11: Bridge Assessment output tab of ODOTApp application software.

The validation of the ODOTApp application software was extremely important in order to check if the methods and algorithms proposed and followed in this research are working properly in estimating the load and condition rating of a bridge. Therefore, the

ODOTApp application software was used to determine the load and condition ratings of the Trumbull County bridge TRU-45.1699 (TRU Bridge). The input data were taken from the bridge design and construction plans provided by ODOT, and the truck parameters were recorded on site (truck data shown in Appendix A). The dynamic response data of TRU Bridge were captured using the wireless sensor networks under a 43,100 lb truck at 10 and 25 mph. The Input Parameters tab is shown in Fig. 4-12 after all inputs including bridge dynamic response. By going to the Bridge Assessment tab and performing the analysis, the results of load and condition ratings were 13.69 and 8, respectively, as shown in Fig. 4-13. These results were close to ODOT’s ratings. After on-site validation, the researchers believe that the application software can be used to instantly estimate the load and condition ratings of a bridge on site.

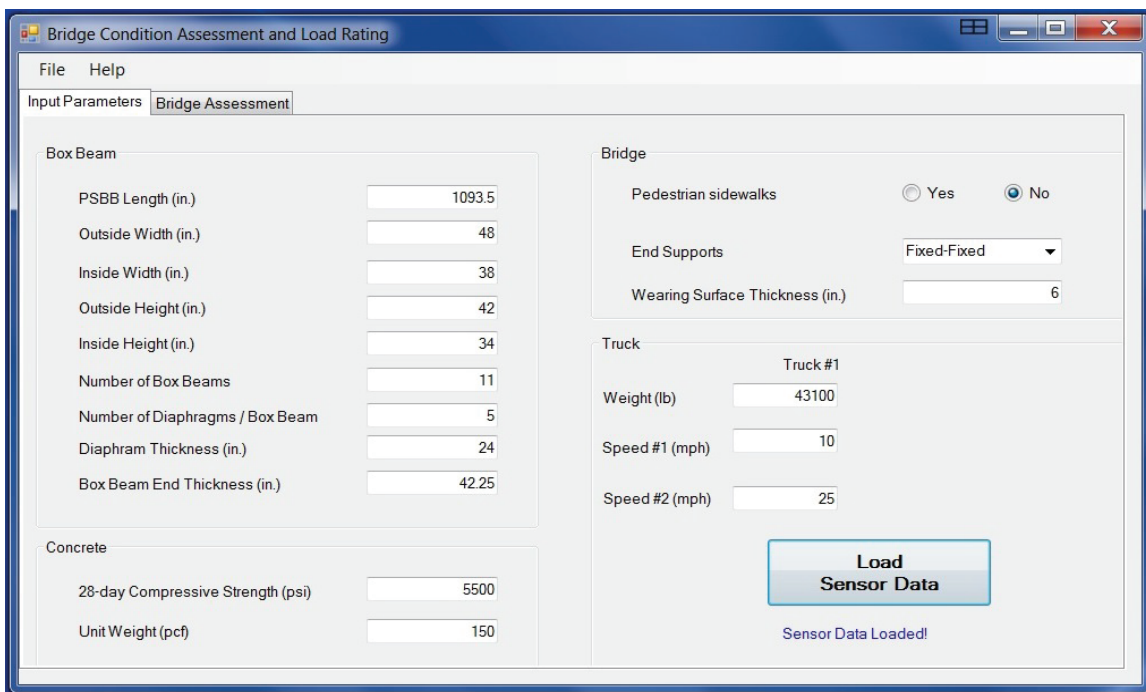


Figure 4-12: Input Parameters tab of ODOTApp with TRU Bridge response.

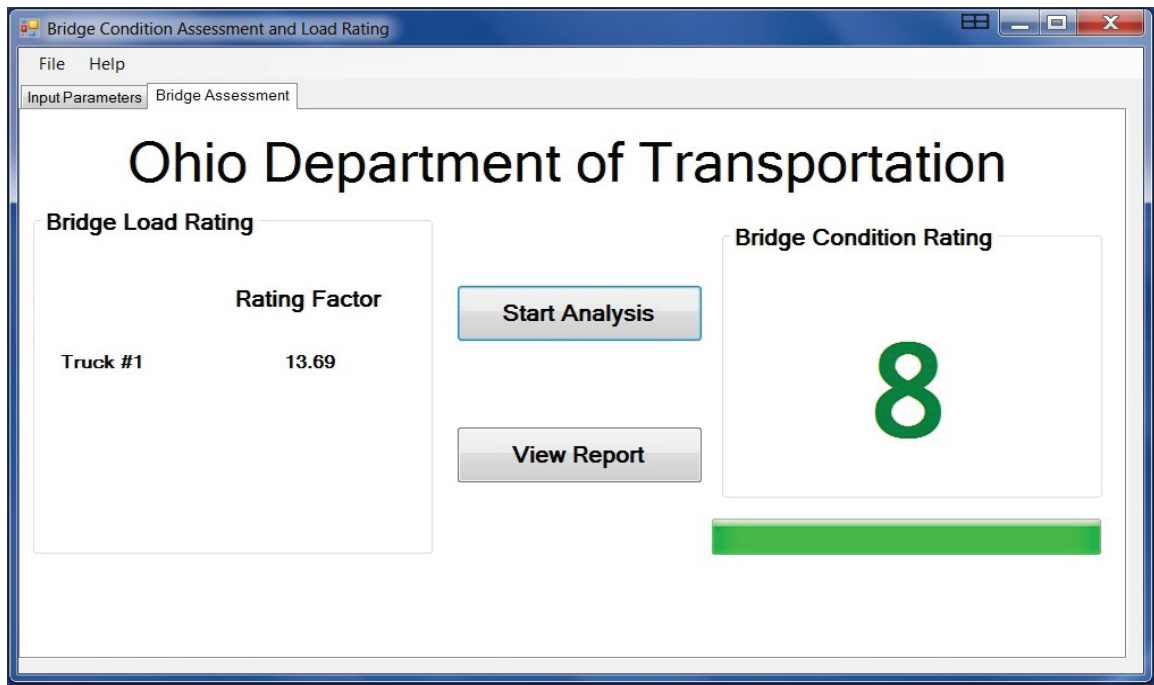


Figure 4-13: Bridge Assessment tab of ODOTApp with TRU Bridge response.

This research performed the load rating of a PSBB bridge using its dynamic response under vehicular loads collected through wireless sensor networks. A parallel research was also performed by another graduate student to estimate the condition rating of a PSBB bridge using its dynamic response collected using the same procedure. The application software herein was developed based on the combined results and algorithms of both studies. As a result, the application software described herein includes both load rating and condition rating of a bridge. In fact, the combined application software will be more economical compared to a standalone product.

## CHAPTER 5

### Conclusions and Recommendations

#### 5.1 Conclusions

Although the percentage of bridges, which is either functionally obsolete or structurally deficient, has been declining slowly over the last decade, a significant portion is closed to traffic or posted for load restrictions. For posting load limits, the load bearing capacity of bridges needs to be evaluated. Considering the fact that the current theoretical load rating of bridges is a very conservative approach and sometimes proposes capacity well below the actual structural capacity, this research was aimed at developing a state-of-the-art method and application software for load rating of single-span prestressed box beam bridges based on their dynamic response under vehicular loads collected through wireless sensor networks. The load rating method includes analyzing the collected dynamic response using FFT and peak picking algorithms to determine the maximum peak amplitude and its corresponding frequency. Using the SDOF method and the load displacement relationship along with the analysis data and bridge geometric properties, bridge bending stiffness can be calculated and used to estimate its load bearing capacity.

Using the results from the ATB Bridge finite element model, it has been found that the vibration frequency at the dominant peak amplitude under vehicular loads is the first bending frequency of the bridge. Therefore, this first bending frequency of ATB Bridge was used to determine the bending stiffness in its current condition and estimate its load bearing capacity. The load ratings of ATB Bridge estimated from this research were compared to those using BARS and VIRTIS. The gross weight and axle spacing of

the two-axle Fully-loaded Truck used for data collection are 16.15 tons and 14.75 ft, respectively. The load rating of ATB Bridge for this truck was estimated as 67 tons. On the other hand, BARS and VIRTIS load ratings of ATB Bridge for OH-2F1 truck, which weighs around 15 tons with 10 ft axle spacing, were 73 and 71 tons, respectively. These two trucks are almost identical considering their gross weights and axle spacing. Therefore, the load rating method developed herein generates acceptable load ratings of a bridge. This cost-effective application software for load rating is expected to help ODOT save time and money for bridge maintenance. This method and the application software can supplement but in no way can replace the current methods without further research with more bridges. A database of PSBB bridge dynamic response may be developed and incorporated into the application software to make it more robust and accurate.

## **5.2 Recommendations**

This research coalesces bridge response and wireless sensor technology in health monitoring, and reinforces the possibility of bridge load rating using its dynamic response. More studies are needed to establish the proposed algorithms as replacements for other expensive and time-consuming tools and methods for other types of bridges. Future studies should include testing multiple-span bridges with various geometrics and materials. The effect of multiple trucks passing over the bridge might be investigated as well. In lieu of wireless SunSPOT sensors, other types of accelerometer sensor including tethered sensor networks might be used to verify and check the effectiveness of the proposed WSN technology. The load rating with sensors relocated on the bridge centerline should be investigated as well to find out difference, if any, from the proposed



sensor location. In addition, the dynamic response of bridges could be used to investigate substructure conditions of a bridge after an extreme event, such as an earthquake.

## REFERENCES

1. American Society of Civil Engineers (ASCE, 2013). "Report Card for America's Infrastructure", 1801 Alexander Bell Drive, Reston, Virginia.
2. Lichtenstein, A. (1993). "Bridge Rating Through Non-Destructive Load Testing", Final Draft, NCHRP Report 12-28(13)A, Transportation Research Board, Washington, D.C.
3. U.S. Department of Transportation (USDOT, 2012). "Transportation Statistics Annual Report", Bureau of Transportation Statistics, (2012) Table 1-28: Condition of U.S. Highway Bridges. URL as of 10/16/2013: <[http://www.rita.dot.gov/bts/sites/rita.dot.gov/bts/files/publications/national\\_transportation\\_statistics/index.html#chapter\\_1](http://www.rita.dot.gov/bts/sites/rita.dot.gov/bts/files/publications/national_transportation_statistics/index.html#chapter_1)>
4. American Association of State Highway and Transportation Officials (AASHTO, 2008). "Bridging the Gap." American Association of State Highway and Transportation Officials, 444 North Capitol Street, NW Suite 249 Washington, DC 20001.
5. Transportation for Tomorrow (2007). "Report of the National Surface Transportation Policy (NSTP) and Revenue Study Commission." Final report, Volume II, Chapter 4, pp. 6.
6. Russell, H. G. (2008). "Adjacent Precast Box Beam Bridges: Connection Details", NCHRP Synthesis 20-05/ Topic 39-10.
7. PCI State-of-the-Practice (SOP-02-2011). "Report of precast/prestressed adjacent box beam bridges", PCI Committee on Bridges, Precast/Prestressed Concrete

Institute, ISBN 978-0-9846705-2.

8. Bridge Design Manual (BDM, 2011). Ohio Department of Transportation, Columbus, Ohio.
9. U.S. Department of Transportation, Federal Highway Administration (2012). “Deficient Bridges by State and Highway System”, URL as of 10/16/2013: <[www.fhwa.dot.gov/bridge/deficient.cfm](http://www.fhwa.dot.gov/bridge/deficient.cfm)>
10. Manual of Bridge Inspection (MBI, 2010). Ohio Department of Transportation, Columbus, Ohio.
11. Balageas, D., Fritzen, C. P., and Guemes, A. (2006). “Structural Health Monitoring.” ISTE USA, 4308 Patrice Road, Newport Beach, CA 92663.
12. Straser, E. G. and Kiremidjian, A. S. (1998). “A modular, wireless damage monitoring system for structures.” John A. Blume Center Technical Report No. 128, Stanford University, Stanford, CA.
13. Kim, S., Pakzad, S., Culler, D., Demmel, J., Fenves, G., Glaser, S., and Turon, M. (2007). “Health Monitoring of Civil Infrastructures Using Wireless Sensor Networks.” Proceedings of the 6th International Conference on Information Processing in Sensor Networks (IPSN '07), Cambridge, MA, ACM Press, pp.254-263.
14. Gangone, M. V., Whelan, M. J., Janoyan, K. D., and Jha, R. (2008). “Field deployment of a dense wireless sensor network for condition assessment of a bridge superstructure.” SPIE Smart Structures Symposium, San Diego, California.
15. Barker, R. M. and Puckett, J. A. (2007). “Design of Highway Bridges an LRFD

- Approach SECOND EDITION.” John Wiley & Sons, Inc., Hoboken, New Jersey.
16. Chen, S. E., Siswobusono, P., Delatte, N., and Stephens B. J. (2002). "Feasibility Study on Dynamic Bridge Load Rating," University Transportation Center for Alabama, (UTCA).
  17. Samali, B., Crews, K., Jianchun, Li, Bakoss, S., and Champion, C. (2003). "Assessing the Load Carrying Capacity of Timber Bridges using Dynamic Methods." Institute of Public Works Engineering Australia, Sydney, Australia.
  18. Chowdhury, M. R. (1999). "Rapid Beam Load Capacity Assessment Using Dynamic Measurements." Research Structural Engineering, Structures Laboratory, U.S. Army Engineering Waterways Experimental Station, Vicksburg, MS 39180-6199.
  19. Google Maps (2013). URL as of 10/16/2013:  
<<http://maps.google.com/maps?hl=en&tab=w1>>
  20. Oracle Corporation (2012). Sun SPOT World URL:  
<<http://www.sunspotworld.com/Tutorial/index.html>>
  21. Logan, D. L. (2001). "A first Course in the Finite Element Method Using Algor"
  22. SIMULIA ABAQUS 6.12-1 Documentation (2013). URL as of 10/16/2013:  
<<http://ts06983:2080/V6.12/index.html>>
  23. Building Code Requirements for Structural Concrete and Commentary, ACI 318-08 (2008). American Concrete Institute, 38800 Country Club Drive, Farmington Hills, MI 48331.
  24. AASHTO LRFD Bridge Design Specifications (AASHTO, 2007). American Association of State Highway and Transportation Officials, 444 North Capitol

Street, NW Suite 249 Washington, DC 20001.

25. Prestressed Concrete Bridge (48") CBP2, Ohio Department of Transportation,

(1972) URL as of 10/16/2013:

<<http://www.dot.state.oh.us/Divisions/Engineering/Structures/standard/ArchivedStandardDrawings/Pages/ConcreteBeam%28prestressed%29.aspx>>

26. Tedesco, J. W., McDougal, W. G., and Ross, C. A. (1999). "Structural Dynamics Theory and Applications", Addison-Wesley Longman Inc. Menlo Park, CA.

27. Cooley, J. W. and Tukey, J. W. (1965). "An algorithm for the machine calculation of complex Fourier series." IBM Watson Research Center, Yorktown Heights, NY; Bell Telephone Laboratories, Murray Hill; and Princeton University, NJ.

28. AASHTOWare Bridge Analytical Software (AASHTO, 2013). URL as of 10/16/2013: < <http://www.aashtoware.org/Bridge/Pages/Rating.aspx?PID=3>>

29. Ohio Department of Transportation (ODOT, 2013). "Bridge Design Manual", Columbus, Ohio.

# APPENDICES

## Appendix A

### Trucks Information, Axle Dimensions and Weights

Truck axle loads and dimensions for MAH Bridge:



OHIO DEPARTMENT OF PUBLIC SAFETY  
OHIO STATE HIGHWAY PATROL

#### Portable Scale Arrest and Weight Record

Date/Time of Violation \_\_\_\_\_ @ \_\_\_\_\_ Date/Time Vehicle Weighed 11-5-12 @ 0810  
 Violation Occurred at \_\_\_\_\_ Distance Traveled \_\_\_\_\_  
 Vehicle Weighed at ODOT BAILEY RD County of Arrest \_\_\_\_\_  
 Citation Number \_\_\_\_\_ Court Date \_\_\_\_\_ Total Fine Including Court Costs \_\_\_\_\_  
 Driver Name \_\_\_\_\_ Operator License # \_\_\_\_\_ State \_\_\_\_\_  
 Carrier Name ODOT Description of Load EMPTY  
 Power Unit: Make INTL Model Year 99 Color WH Style of Vehicle DUMP  
 Registration: Power Unit T4827 State \_\_\_\_\_ Trailer \_\_\_\_\_ State \_\_\_\_\_

#### Reasonable Suspicion for Traffic Stop (check all that apply)

- Bulging Tires   
  Visible Load   
  Pulling Hard   
  Slow Speed   
  Insecure Load   
  Vehicle Defect  
 Oversize Load (5577.05)   
  Registration Violation   
  Other Violation \_\_\_\_\_

Axles	Axle Spacing	Scale #	Axle #	Left	Right	Axle #	Scale #	Total Weight
		<u>131</u>	Steer	<u>4,000</u>	<u>3,900</u>	Steer	<u>129</u>	<u>7,900</u>
1-2	<u>11-7</u>	<u>139</u>	2	<u>5,500</u>	<u>5,200</u>	2	<u>115</u>	<u>10,700</u>
1-3			3			3		
1-4			4			4		
1-5			5			5		
1-6			6			6		
1-7			7			7		
1-8			8			8		
1-9			9			9		
1-10			10			10		
1-11			11			11		

5577.04 (B) Maximum Gross Weight Allowed \_\_\_\_\_ lbs    5577.04 (D) Maximum Gross Weight Allowed \_\_\_\_\_ lbs

	Actual Weight in Pounds	Allowed Weight in Pounds	Number of Pounds Overweight	Issued Citation
Gross Weight	<u>18,600</u>	<u>40,000</u>		<input type="checkbox"/>
Axles 1	<u>7,900</u>	<u>20,000</u>		<input type="checkbox"/>
Axles 2	<u>10,700</u>	<u>20,000</u>		<input type="checkbox"/>
Inner-Bridge				<input type="checkbox"/>

Vehicle Length 11 Ft 9 In   
 Vehicle Width 6 Ft 0 In   
 Vehicle Height \_\_\_\_\_ Ft \_\_\_\_\_ In  
 Arresting Officer \_\_\_\_\_ Unit \_\_\_\_\_ LLI Unit # 432 LLI Unit # \_\_\_\_\_  
 Level Checked By 3022 Unit \_\_\_\_\_ All Scales Department of Agriculture Sealed  Yes  No  
 Disposition of Vehicle: Axles shifted  Vehicle off loaded  Driven to closest safe haven to get legal   
 Other  (Explain) \_\_\_\_\_  
 Check box for citations issued (check all that apply): Oversize  IFTA  Unsafe  Permit Violation   
 Other Arrest  (List all) \_\_\_\_\_



OHIO DEPARTMENT OF PUBLIC SAFETY  
OHIO STATE HIGHWAY PATROL

Portable Scale Arrest and Weight Record

Date/Time of Violation \_\_\_\_\_ @ \_\_\_\_\_ Date/Time Vehicle Weighed 11-5-12 @ 0746  
Violation Occurred at \_\_\_\_\_ Distance Traveled \_\_\_\_\_  
Vehicle Weighed at ODOT Bailey Rd County of Arrest \_\_\_\_\_  
Citation Number \_\_\_\_\_ Court Date \_\_\_\_\_ Total Fine Including Court Costs \_\_\_\_\_  
Driver Name \_\_\_\_\_ Operator License # \_\_\_\_\_ State \_\_\_\_\_  
Carrier Name ODOT Description of Load 1/2 LOAD  
Power Unit: Make INJL Model Year 07 Color WHI Style of Vehicle Dump  
Registration: Power Unit T4577 State \_\_\_\_\_ Trailer \_\_\_\_\_ State \_\_\_\_\_

Reasonable Suspicion for Traffic Stop (check all that apply)

- Bulging Tires  Visible Load  Pulling Hard  Slow Speed  Insecure Load  Vehicle Defect  
 Oversize Load (5577.05)  Registration Violation  Other Violation \_\_\_\_\_

Axes	Axle Spacing	Scale #	Axle #	Left	Right	Axle #	Scale #	Total Weight
		<u>131</u>	Steer	<u>5,600</u>	<u>5,800</u>	Steer	<u>129</u>	<u>11,400</u>
1-2	<u>17-8</u>	<u>139</u>	2	<u>9,600</u>	<u>10,100</u>	2	<u>115</u>	<u>19,700</u>
1-3			3			3		
1-4			4			4		
1-5			5			5		
1-6			6			6		
1-7			7			7		
1-8			8			8		
1-9			9			9		
1-10			10			10		
1-11			11			11		

5577.04 (B) Maximum Gross Weight Allowed \_\_\_\_\_ lbs 5577.04 (D) Maximum Gross Weight Allowed \_\_\_\_\_ lbs

	Actual Weight in Pounds	Allowed Weight in Pounds	Number of Pounds Overweight	Issued Citation
Gross Weight	<u>31,100</u>	<u>40,000</u>		<input type="checkbox"/>
Axes 1	<u>11,400</u>	<u>20,000</u>		<input type="checkbox"/>
Axes 2	<u>19,700</u>	<u>20,000</u>		<input type="checkbox"/>
Inner-Bridge				<input type="checkbox"/>

Vehicle Length 14 Ft 8 In Vehicle Width 6 Ft 0 In Vehicle Height \_\_\_\_\_ Ft \_\_\_\_\_ In  
Arresting Officer \_\_\_\_\_ Unit \_\_\_\_\_ LLI Unit # 432 LLI Unit # \_\_\_\_\_  
Level Checked By 3022 Unit \_\_\_\_\_ All Scales Department of Agriculture Sealed  Yes  No  
Disposition of Vehicle: Axles shifted  Vehicle off loaded  Driven to closest safe haven to get legal   
Other  (Explain) \_\_\_\_\_  
Check box for citations issued (check all that apply): Oversize  IFTA  Unsafe  Permit Violation   
Other Arrest  (List all) \_\_\_\_\_



OHIO DEPARTMENT OF PUBLIC SAFETY  
OHIO STATE HIGHWAY PATROL

Portable Scale Arrest and Weight Record

Date/Time of Violation \_\_\_\_\_ @ \_\_\_\_\_ Date/Time Vehicle Weighed 11-5-12 @ 0834  
Violation Occurred at \_\_\_\_\_ Distance Traveled \_\_\_\_\_  
Vehicle Weighed at 0001 BAILEY RD County of Arrest \_\_\_\_\_  
Citation Number \_\_\_\_\_ Court Date \_\_\_\_\_ Total Fine Including Court Costs \_\_\_\_\_  
Driver Name \_\_\_\_\_ Operator License # \_\_\_\_\_ State \_\_\_\_\_  
Carrier Name ONOT Description of Load FULL LOAD  
Power Unit: Make INTL Model Year 08 Color WHITE Style of Vehicle Dump  
Registration: Power Unit F 4 946 State \_\_\_\_\_ Trailer \_\_\_\_\_ State \_\_\_\_\_

Reasonable Suspicion for Traffic Stop (check all that apply)

- Bulging Tires  Visible Load  Pulling Hard  Slow Speed  Insecure Load  Vehicle Defect  
 Oversize Load (5577.05)  Registration Violation  Other Violation \_\_\_\_\_

Axles	Axle Spacing	Scale #	Axle #	Left	Right	Axle #	Scale #	Total Weight
		<u>131</u>	Steer	<u>6,000</u>	<u>5,900</u>	Steer	<u>129</u>	<u>11,900</u>
1-2	<u>14-9</u>	<u>139</u>	2	<u>13,900</u>	<u>13,700</u>	2	<u>115</u>	<u>27,600</u>
1-3			3			3		
1-4			4			4		
1-5			5			5		
1-6			6			6		
1-7			7			7		
1-8			8			8		
1-9			9			9		
1-10			10			10		
1-11			11			11		

5577.04 (B) Maximum Gross Weight Allowed \_\_\_\_\_ lbs 5577.04 (D) Maximum Gross Weight Allowed \_\_\_\_\_ lbs

	Actual Weight In Pounds	Allowed Weight In Pounds	Number of Pounds Overweight	Issued Citation
Gross Weight	<u>39,500</u>	<u>40,000</u>		<input type="checkbox"/>
Axles 1	<u>11,900</u>	<u>20,000</u>		<input type="checkbox"/>
Axles 2	<u>27,600</u>	<u>20,000</u>		<input type="checkbox"/>
Inner-Bridge				<input type="checkbox"/>

Vehicle Length 14 Ft 9 In Vehicle Width 6 Ft 0 In Vehicle Height \_\_\_\_\_ Ft \_\_\_\_\_ In  
Arresting Officer \_\_\_\_\_ Unit \_\_\_\_\_ LLI Unit # 432 LLI Unit # \_\_\_\_\_  
Level Checked By 3022 Unit \_\_\_\_\_ All Scales Department of Agriculture Sealed  Yes  No  
Disposition of Vehicle: Axles shifted  Vehicle off loaded  Driven to closest safe haven to get legal   
Other  (Explain) \_\_\_\_\_  
Check box for citations issued (check all that apply): Oversize  IFTA  Unsafe  Permit Violation   
Other Arrest  (List all) \_\_\_\_\_



Truck axle loads and dimensions for ATB Bridge:



OHIO DEPARTMENT OF PUBLIC SAFETY  
OHIO STATE HIGHWAY PATROL

**Portable Scale Arrest and Weight Record**

Date/Time of Violation \_\_\_\_\_ @ \_\_\_\_\_ Date/Time Vehicle Weighed 11-13-12 @ 0828  
 Violation Occurred at \_\_\_\_\_ Distance Traveled \_\_\_\_\_  
 Vehicle Weighed at ODOT 512322 County of Arrest \_\_\_\_\_  
 Citation Number \_\_\_\_\_ Court Date \_\_\_\_\_ Total Fine Including Court Costs \_\_\_\_\_  
 Driver Name \_\_\_\_\_ Operator License # \_\_\_\_\_ State \_\_\_\_\_  
 Carrier Name ODOT Description of Load EMPTY  
 Power Unit: Make INTL Model Year 06 Color WHI Style of Vehicle Dump  
 Registration: Power Unit T4614 State OH Trailer \_\_\_\_\_ State \_\_\_\_\_

Reasonable Suspicion for Traffic Stop (check all that apply)

- Bulging Tires  Visible Load  Pulling Hard  Slow Speed  Insecure Load  Vehicle Defect  
 Oversize Load (5577.05)  Registration Violation  Other Violation \_\_\_\_\_

Axles	Axle Spacing	Scale #	Axle #	Left	Right	Axle #	Scale #	Total Weight
		<u>142</u>	Steer	<u>5,100</u>	<u>4,900</u>	Steer	<u>139</u>	<u>10,000</u>
1-2	<u>14-10</u>	<u>144</u>	2	<u>5,100</u>	<u>4,400</u>	2	<u>115</u>	<u>9,500</u>
1-3			3			3		
1-4			4			4		
1-5			5			5		
1-6			6			6		
1-7			7			7		
1-8			8			8		
1-9			9			9		
1-10			10			10		
1-11			11			11		

5577.04 (B) Maximum Gross Weight Allowed \_\_\_\_\_ lbs 5577.04 (D) Maximum Gross Weight Allowed \_\_\_\_\_ lbs

	Actual Weight in Pounds	Allowed Weight in Pounds	Number of Pounds Overweight	Issued Citation
Gross Weight	<u>19,500</u>	<u>40,000</u>		<input type="checkbox"/>
Axles 1	<u>10,000</u>	<u>20,000</u>		<input type="checkbox"/>
Axles 2	<u>9,500</u>	<u>20,000</u>		<input type="checkbox"/>
Inner-Bridge				<input type="checkbox"/>

Vehicle Length 14 Ft 10 In Vehicle Width 6 Ft 0 In Vehicle Height \_\_\_\_\_ Ft \_\_\_\_\_ In  
 Arresting Officer \_\_\_\_\_ Unit \_\_\_\_\_ LLI Unit # 432 LLI Unit # \_\_\_\_\_  
 Level Checked By 3022 Unit \_\_\_\_\_ All Scales Department of Agriculture Sealed  Yes  No  
 Disposition of Vehicle: Axles shifted  Vehicle off loaded  Driven to closest safe haven to get legal   
 Other  (Explain) \_\_\_\_\_  
 Check box for citations issued (check all that apply): Oversize  IFTA  Unsafe  Permit Violation   
 Other Arrest  (List all) \_\_\_\_\_



OHIO DEPARTMENT OF PUBLIC SAFETY  
OHIO STATE HIGHWAY PATROL

**Portable Scale Arrest and Weight Record**

Date/Time of Violation \_\_\_\_\_ @ \_\_\_\_\_ Date/Time Vehicle Weighed 11-13-12 @ 0824  
 Violation Occurred at \_\_\_\_\_ Distance Traveled \_\_\_\_\_  
 Vehicle Weighed at 0001-52322 County of Arrest \_\_\_\_\_  
 Citation Number \_\_\_\_\_ Court Date \_\_\_\_\_ Total Fine Including Court Costs \_\_\_\_\_  
 Driver Name \_\_\_\_\_ Operator License # \_\_\_\_\_ State \_\_\_\_\_  
 Carrier Name OOOT Description of Load SALT - HALF LOAD  
 Power Unit: Make JNL Model Year 05 Color WHI Style of Vehicle DAMP  
 Registration: Power Unit T4947 State OH Trailer \_\_\_\_\_ State \_\_\_\_\_

Reasonable Suspicion for Traffic Stop (check all that apply)

- Bulging Tires  Visible Load  Pulling Hard  Slow Speed  Insecure Load  Vehicle Defect  
 Oversize Load (5577.05)  Registration Violation  Other Violation \_\_\_\_\_

Axles	Axle Spacing	Scale #	Axle #	Left	Right	Axle #	Scale #	Total Weight
		<u>162</u>	Steer	<u>5,500</u>	<u>5,500</u>	Steer	<u>139</u>	<u>11,000</u>
1-2	<u>14-10</u>	<u>144</u>	2	<u>7,800</u>	<u>8,300</u>	2	<u>115</u>	<u>16,100</u>
1-3			3			3		
1-4			4			4		
1-5			5			5		
1-6			6			6		
1-7			7			7		
1-8			8			8		
1-9			9			9		
1-10			10			10		
1-11			11			11		

5577.04 (B) Maximum Gross Weight Allowed \_\_\_\_\_ lbs 5577.04 (D) Maximum Gross Weight Allowed \_\_\_\_\_ lbs

	Actual Weight in Pounds	Allowed Weight in Pounds	Number of Pounds Overweight	Issued Citation
Gross Weight	<u>27,100</u>	<u>40,000</u>		<input type="checkbox"/>
Axles 1	<u>11,000</u>	<u>20,000</u>		<input type="checkbox"/>
Axles 2	<u>14,100</u>	<u>20,000</u>		<input type="checkbox"/>
Inner-Bridge				<input type="checkbox"/>

Vehicle Length 14 Ft 10 In Vehicle Width 6 Ft 0 In Vehicle Height \_\_\_\_\_ Ft \_\_\_\_\_ In  
 Arresting Officer 432 Unit \_\_\_\_\_ LLI Unit # \_\_\_\_\_ LLI Unit # \_\_\_\_\_  
 Level Checked By 3022 Unit \_\_\_\_\_ All Scales Department of Agriculture Sealed  Yes  No  
 Disposition of Vehicle: Axles shifted  Vehicle off loaded  Driven to closest safe haven to get legal   
 Other  (Explain) \_\_\_\_\_  
 Check box for citations issued (check all that apply): Oversize  IFTA  Unsafe  Permit Violation   
 Other Arrest  (List all) \_\_\_\_\_



OHIO DEPARTMENT OF PUBLIC SAFETY  
OHIO STATE HIGHWAY PATROL

**Portable Scale Arrest and Weight Record**

Date/Time of Violation \_\_\_\_\_ @ \_\_\_\_\_ Date/Time Vehicle Weighed 11-13-12 @ 0817  
 Violation Occurred at \_\_\_\_\_ Distance Traveled \_\_\_\_\_  
 Vehicle Weighed at ODOT-51322 County of Arrest \_\_\_\_\_  
 Citation Number \_\_\_\_\_ Court Date \_\_\_\_\_ Total Fine Including Court Costs \_\_\_\_\_  
 Driver Name \_\_\_\_\_ Operator License # \_\_\_\_\_ State \_\_\_\_\_  
 Carrier Name 712 ODOT Description of Load Full Load  
 Power Unit: Make FMTL Model Year 04 Color WHITE Style of Vehicle Dump  
 Registration: Power Unit T4942 State OH Trailer \_\_\_\_\_ State \_\_\_\_\_

Reasonable Suspicion for Traffic Stop (check all that apply)

- Bulging Tires  Visible Load  Pulling Hard  Slow Speed  Insecure Load  Vehicle Defect  
 Oversize Load (5577.05)  Registration Violation  Other Violation \_\_\_\_\_

Axes	Axle Spacing	Scale #	Axle #	Left	Right	Axle #	Scale #	Total Weight
1-2	14-9	162	Steer 2	6000	5300	Steer 2	139	11,300
1-3		144	3	10,200	10,800	3	115	21,000
1-4			4			4		
1-5			5			5		
1-6			6			6		
1-7			7			7		
1-8			8			8		
1-9			9			9		
1-10			10			10		
1-11			11			11		

5577.04 (B) Maximum Gross Weight Allowed \_\_\_\_\_ lbs 5577.04 (D) Maximum Gross Weight Allowed \_\_\_\_\_ lbs

	Actual Weight in Pounds	Allowed Weight in Pounds	Number of Pounds Overweight	Issued Citation
Gross Weight	32,300	40,000		<input type="checkbox"/>
Axles 1	11,300	20,000		<input type="checkbox"/>
Axles 2	21,000	20,000		<input type="checkbox"/>
Inner-Bridge				<input type="checkbox"/>

Vehicle Length 14 Ft 9 In Vehicle Width 6 Ft 0 In Vehicle Height \_\_\_\_\_ Ft \_\_\_\_\_ In  
 Arresting Officer \_\_\_\_\_ Unit \_\_\_\_\_ LLI Unit # 432 LLI Unit # \_\_\_\_\_  
 Level Checked By 3022 Unit \_\_\_\_\_ All Scales Department of Agriculture Sealed  Yes  No  
 Disposition of Vehicle: Axles shifted  Vehicle off loaded  Driven to closest safe haven to get legal   
 Other  (Explain) \_\_\_\_\_  
 Check box for citations issued (check all that apply): Oversize  IFTA  Unsafe  Permit Violation   
 Other Arrest  (List all) \_\_\_\_\_

Truck axle loads and dimensions for TRU Bridge:



OHIO DEPARTMENT OF PUBLIC SAFETY  
OHIO STATE HIGHWAY PATROL

**Portable Scale Arrest and Weight Record**

Date/Time of Violation 09-27-13 @ NA Date/Time Vehicle Weighed 09-27-13 @ 1045  
 Violation Occurred at SR 45 AT SR 88 Distance Traveled - 0 -  
 Vehicle Weighed at SR 45/NORTH OF SR 88 County of Arrest TRUMBULL  
 Citation Number NA Court Date NA Total Fine Including Court Costs NA  
 Driver Name NA Operator License # NA State NA  
 Carrier Name O.D.O.T. Description of Load GRINDINGS  
 Power Unit: Make INTER Model Year 2012 Color WHITE Style of Vehicle DUMP  
 Registration: Power Unit T 4823 State OHIO Trailer NA State NA

Reasonable Suspicion for Traffic Stop (check all that apply)

- Bulging Tires    Visible Load    Pulling Hard    Slow Speed    Insecure Load    Vehicle Defect  
 Oversize Load (5577.05)    Registration Violation    Other Violation YSU TEST

Axes	Axle Spacing	Scale #	Axle #	Left	Right	Axle #	Scale #	Total Weight
		<u>115</u>	Steer	<u>5,850</u>	<u>6,850</u>	Steer	<u>160</u>	<u>12,700</u>
1-2	<u>146</u>	<u>153</u>	2	<u>15,450</u>	<u>14,950</u>	2	<u>128</u>	<u>30,400</u>
1-3			3			3		
1-4			4			4		
1-5			5			5		
1-6			6			6		
1-7			7			7		
1-8			8			8		
1-9			9			9		
1-10			10			10		
1-11			11			11		

5577.04 (B) Maximum Gross Weight Allowed 40,000 lbs    5577.04 (D) Maximum Gross Weight Allowed 40,000 lbs

★

	Actual Weight in Pounds	Allowed Weight in Pounds	Number of Pounds Overweight	Issued Citation
Gross Weight	<u>43,100</u>	<u>40,000</u>	<u>3,100</u>	<input type="checkbox"/>
Axles				<input type="checkbox"/>
Axles REAR	<u>30,400</u>	<u>20,000</u>	<u>10,400</u>	<input type="checkbox"/>
Inner-Bridge				<input type="checkbox"/>

Vehicle Length      Ft      In    Vehicle Width      Ft      In    Vehicle Height      Ft      In  
 Arresting Officer TP L.S. Woodward Unit 673 LLI Unit # 3022 LLI Unit #       
 Level Checked By 3022 Unit      All Scales Department of Agriculture Sealed  Yes  No  
 Disposition of Vehicle: Axles shifted  Vehicle off loaded  Driven to closest safe haven to get legal   
 Other  (Explain)       
 Check box for citations issued (check all that apply): Oversize  IFTA  Unsafe  Permit Violation   
 Other Arrest  (List all)

## Appendix B

### Collected Data and Load Rating Calculations of ATB Bridge

ATB Bridge acceleration data under Fully-loaded Truck at 25 mph

Sensor #1		Sensor #2		Sensor #3		Sensor #4	
Time (msec)	Acceleration (g)	Time (msec)	Acceleration (g)	Time (msec)	Acceleration (g)	Time (msec)	Acceleration (g)
0	0	0	0	1	0	0	0.01563
10	-0.0156	10	-0.015625	10	0	10	0.03125
20	0	20	0	20	0.015625	20	0.01563
30	0	30	0.015625	30	0.015625	30	0.03125
40	0	40	0	40	0.015625	40	0.01563
50	0	50	0.015625	50	0	50	0.03125
60	-0.0156	60	-0.015625	60	0	60	0
70	-0.0313	70	0.015625	70	0	70	0.01563
80	0.01563	80	0.03125	80	0.015625	80	0.01563
90	0.01563	90	0.015625	90	0.015625	90	0.01563
100	-0.0156	100	0	100	0.015625	100	0.03125
110	0	110	0	110	0.03125	110	0.01563
120	0	120	0.03125	120	0.015625	120	0.03125
130	0	130	0	130	0.015625	130	0.03125
140	0	140	0	140	-0.015625	140	0
150	-0.0156	150	0	150	0.03125	150	0.01563
160	0.01563	160	0	160	0	160	0.04688
170	0	174	0.03125	174	0	170	0
180	-0.0313	180	0.015625	181	0.015625	184	0.01563
190	0	190	0	190	0.03125	190	0.03125
200	0	200	0.03125	200	0.015625	200	0
.....	.....	.....	.....	.....	.....	.....	.....
.....	.....	.....	.....	.....	.....	.....	.....

ATB Bridge model acceleration data under Fully-loaded Truck at 25 mph

Sensor #1		Sensor #2		Sensor #3		Sensor #4	
Time (msec)	Acceleration (g)	Time (msec)	Acceleration (g)	Time (msec)	Acceleration (g)	Time (msec)	Acceleration (g)
0	-1	0	-0.9999986	0	-1.0000013	0	-1
0.01	-1.33941	0.01	-2.4210129	0.01	-0.6754006	0.01	-1.0626
0.02	2.863717	0.02	-4.2600088	0.02	-0.1303344	0.02	-1.53078
0.03	-1.59082	0.03	-1.734302	0.03	-0.5599596	0.03	-0.49705
0.04	-2.1777	0.04	0.11662557	0.04	-0.8557031	0.04	-1.40808
0.05	-0.18549	0.05	0.31286295	0.05	1.7007868	0.05	0.231656
0.06	-3.79851	0.06	0.68159297	0.06	-1.7314424	0.06	2.692012
0.07	-0.16237	0.07	4.49513185	0.07	0.63683184	0.07	3.990912
0.08	0.515303	0.08	3.31101443	0.08	0.44790485	0.08	0.520151
0.09	3.200698	0.09	-1.5487406	0.09	4.02153726	0.09	2.686225
0.1	-0.08493	0.1	3.44664106	0.1	-2.3583765	0.1	-0.17328
0.11	2.81004	0.11	3.70786931	0.11	1.84954973	0.11	-0.57674
0.12	-1.38704	0.12	-0.9725098	0.12	-3.6362939	0.12	0.891428
0.13	-6.83073	0.13	1.59731326	0.13	-5.3822292	0.13	-2.30483
0.14	2.013323	0.14	-4.1706794	0.14	-1.205504	0.14	2.042213
0.15	0.790555	0.15	-4.8211799	0.15	-2.5130865	0.15	-3.06275
0.16	-4.50665	0.16	1.59905775	0.16	-3.359907	0.16	-1.54987
0.17	0.29366	0.17	-3.8708992	0.17	0.5515159	0.17	-2.98925
0.18	-0.69055	0.18	-0.406506	0.18	-0.3205951	0.18	-2.59804
0.19	-1.20416	0.19	-0.9300374	0.19	-2.3111066	0.19	-2.23722
0.2	-0.80467	0.2	1.75441466	0.2	-1.432016	0.2	-1.52192
0.21	-1.68634	0.21	-2.1842887	0.21	2.04453889	0.21	-0.64741
0.22	2.181287	0.22	-0.2280089	0.22	-1.2437619	0.22	-1.43687
0.23	2.654741	0.23	1.81416245	0.23	4.66441058	0.23	2.200728
0.24	0.490813	0.24	0.29528833	0.24	1.96751328	0.24	4.455553
0.25	1.369262	0.25	-2.8512008	0.25	4.49907923	0.25	-1.25128
....	.....	....	.....	....	.....	....	.....
....	.....	....	.....	....	.....	....	.....

ATB Bridge model displacement data under Fully-loaded Truck at 25mph

Sensor #1		Sensor #2		Sensor #3		Sensor #4	
Time (msec)	Displacement (in)	Time (msec)	Displacement (in)	Time (msec)	Displacement (in)	Time (msec)	Displacement (in)
0	0.006636	0	0.00735788	0	0.00783256	0	0.00806
0.01	-0.01416	0.01	-0.0129933	0.01	-0.0116793	0.01	-0.01103
0.02	-0.06712	0.02	-0.0737669	0.02	-0.0777293	0.02	-0.07946
0.03	-0.1432	0.03	-0.1684619	0.03	-0.1861757	0.03	-0.19506
0.04	-0.24199	0.04	-0.2833486	0.04	-0.3126599	0.04	-0.32754
0.05	-0.34997	0.05	-0.4064143	0.05	-0.4457539	0.05	-0.46548
0.06	-0.4474	0.06	-0.5249617	0.06	-0.5795764	0.06	-0.60699
0.07	-0.52924	0.07	-0.623015	0.07	-0.6897362	0.07	-0.72354
0.08	-0.58944	0.08	-0.6890547	0.08	-0.759419	0.08	-0.79489
0.09	-0.61331	0.09	-0.7178884	0.09	-0.7917923	0.09	-0.82902
0.1	-0.59945	0.1	-0.7057331	0.1	-0.7813618	0.1	-0.81955
0.11	-0.5568	0.11	-0.6520655	0.11	-0.7195573	0.11	-0.75355
0.12	-0.48532	0.12	-0.5655398	0.12	-0.6218505	0.12	-0.65009
0.13	-0.38902	0.13	-0.4566343	0.13	-0.504548	0.13	-0.52869
0.14	-0.28731	0.14	-0.3364302	0.14	-0.3712385	0.14	-0.3886
0.15	-0.19153	0.15	-0.2193872	0.15	-0.238374	0.15	-0.24757
0.16	-0.10522	0.16	-0.1207163	0.16	-0.131132	0.16	-0.13614
0.17	-0.04309	0.17	-0.0499867	0.17	-0.0548781	0.17	-0.05724
0.18	-0.01692	0.18	-0.0149067	0.18	-0.0128399	0.18	-0.01152
0.19	-0.02222	0.19	-0.0214231	0.19	-0.0198976	0.19	-0.01873
0.2	-0.05768	0.2	-0.0673195	0.2	-0.0740841	0.2	-0.07746
0.21	-0.1269	0.21	-0.1462795	0.21	-0.1598024	0.21	-0.16654
0.22	-0.21745	0.22	-0.2504207	0.22	-0.2729395	0.22	-0.28398
0.23	-0.31375	0.23	-0.3679881	0.23	-0.4061485	0.23	-0.42521
0.24	-0.41154	0.24	-0.483185	0.24	-0.5341401	0.24	-0.55995
0.25	-0.50061	0.25	-0.5839254	0.25	-0.6424348	0.25	-0.6717
....	.....	....	.....	....	.....	....	.....
....	.....	....	.....	....	.....	....	.....

Effective flexural rigidity of ATB Bridge

Truck	Speed (mph)	Sensors			
		1	2	3	4
Empty Truck	10	2.154E+12	2.026E+12	2.154E+12	2.856E+12
	15	2.423E+12	2.564E+12	2.287E+12	2.287E+12
	20	1.294E+12	2.212E+12	2.344E+12	1.196E+12
	25	2.344E+12	1.294E+12	1.5E+12	2.344E+12
Half-loaded Truck	10	2.026E+12	1.236E+12	2.154E+12	2.154E+12
	15	2.212E+12	2.344E+12	2.344E+12	2.344E+12
	20	2.154E+12	2.154E+12	2.154E+12	2.154E+12
	25	1.901E+12	1.901E+12	2.564E+12	1.78E+12
Fully-loaded Truck	10	2.154E+12	1.442E+12	2.423E+12	2.154E+12
	15	2.212E+12	2.212E+12	2.212E+12	2.212E+12
	20	2.154E+12	2.154E+12	1.901E+12	2.026E+12
	25	2.154E+12	2.154E+12	2.154E+12	2.154E+12
Truck	Speed (mph)	Sensors			
		5	6	7	8
Empty Truck	10	2.287E+12	2.287E+12	2.287E+12	1.442E+12
	15	2.423E+12	2.423E+12	3.009E+12	2.287E+12
	20	1.722E+12	1.839E+12	1.294E+12	1.839E+12
	25	7.655E+11	1.294E+12	1.196E+12	1.294E+12
Half-loaded Truck	10	2.154E+12	2.154E+12	2.154E+12	2.154E+12
	15	2.344E+12	2.48E+12	2.344E+12	2.344E+12
	20	2.154E+12	2.154E+12	2.154E+12	2.154E+12
	25	1.901E+12	1.901E+12	2.154E+12	2.026E+12
Fully-loaded Truck	10	1.337E+12	1.78E+12	2.154E+12	2.423E+12
	15	2.212E+12	2.212E+12	2.212E+12	2.212E+12
	20	1.551E+12	2.026E+12	1.78E+12	2.154E+12
	25	2.154E+12	2.154E+12	2.154E+12	2.154E+12



Effective stiffness of ATB Bridge

Truck	Speed (mph)	Sensors			
		1	2	3	4
Empty Truck	10	2.154E+12	2.026E+12	2.154E+12	2.856E+12
	15	2.423E+12	2.564E+12	2.287E+12	2.287E+12
	20	1.294E+12	2.212E+12	2.344E+12	1.196E+12
	25	2.344E+12	1.294E+12	1.5E+12	2.344E+12
Half-loaded Truck	10	2.026E+12	1.236E+12	2.154E+12	2.154E+12
	15	2.212E+12	2.344E+12	2.344E+12	2.344E+12
	20	2.154E+12	2.154E+12	2.154E+12	2.154E+12
	25	1.901E+12	1.901E+12	2.564E+12	1.78E+12
Fully-loaded Truck	10	2.154E+12	1.442E+12	2.423E+12	2.154E+12
	15	2.212E+12	2.212E+12	2.212E+12	2.212E+12
	20	2.154E+12	2.154E+12	1.901E+12	2.026E+12
	25	2.154E+12	2.154E+12	2.154E+12	2.154E+12
Truck	Speed (mph)	Sensors			
		5	6	7	8
Empty Truck	10	2.287E+12	2.287E+12	2.287E+12	1.442E+12
	15	2.423E+12	2.423E+12	3.009E+12	2.287E+12
	20	1.722E+12	1.839E+12	1.294E+12	1.839E+12
	25	7.655E+11	1.294E+12	1.196E+12	1.294E+12
Half-loaded Truck	10	2.154E+12	2.154E+12	2.154E+12	2.154E+12
	15	2.344E+12	2.48E+12	2.344E+12	2.344E+12
	20	2.154E+12	2.154E+12	2.154E+12	2.154E+12
	25	1.901E+12	1.901E+12	2.154E+12	2.026E+12
Fully-loaded Truck	10	1.337E+12	1.78E+12	2.154E+12	2.423E+12
	15	2.212E+12	2.212E+12	2.212E+12	2.212E+12
	20	1.551E+12	2.026E+12	1.78E+12	2.154E+12
	25	2.154E+12	2.154E+12	2.154E+12	2.154E+12

Dynamic load factor of acceleration (DLFA)

Truck	Sensors			
	1	2	3	4
Empty Truck	1.33	1.3432161	1.33	1.33
Half-loaded Truck	1.33	1.6302834	2.4381396	1.6579661
Fully-loaded Truck	3.0678407	4.4716457	3.9922631	2.7970285
Truck	Sensors			
	5	6	7	8
Empty Truck	1.33	1.33	1.33	1.7022613
Half-loaded Truck	1.33	1.8731069	2.183615	2.2350217
Fully-loaded Truck	4.1414451	4.177086	3.459431	3.4670745

Load bearing capacity of ATB Bridge

Truck	Speed (mph)	Sensors			
		1	2	3	4
Empty Truck	10	186.81116	173.92899	186.81116	247.70503
	15	210.13727	220.13328	198.30833	198.30833
	20	112.18977	189.96769	203.31162	103.73042
	25	203.31162	111.08592	130.12125	203.31162
Half-loaded Truck	10	175.65731	87.469089	101.90509	149.85762
	15	191.85538	165.86346	110.90606	163.09408
	20	186.81116	152.40224	101.90509	149.85762
	25	164.85696	134.49181	121.27548	123.84927
Fully-loaded Truck	10	80.988185	37.195186	70.006052	88.829572
	15	83.175001	57.063477	63.915541	91.228119
	20	80.988185	55.563178	54.921171	83.525861
	25	80.988185	55.563178	62.235089	88.829572
Truck	Speed (mph)	Sensors			
		5	6	7	8
Empty Truck	10	198.30833	198.30833	198.30833	97.707497
	15	210.13727	210.13727	260.91807	154.941
	20	149.3718	159.48987	112.18977	124.61161
	25	66.387468	112.18977	103.73042	87.655397
Half-loaded Truck	10	186.81116	132.64531	113.78326	111.16619
	15	203.31162	152.72357	123.83339	120.98516
	20	186.81116	132.64531	113.78326	111.16619
	25	164.85696	117.05673	113.78326	104.52884
Fully-loaded Truck	10	37.240087	49.158167	71.820727	80.61049
	15	61.613192	61.087478	73.760007	73.597395
	20	43.191737	55.929951	59.355973	71.662391
	25	59.993274	59.481382	71.820727	71.662391

## Appendix C

### FE Model Validation

Two analyses were performed to validate the ATB Bridge model. The results of these analyses were compared to the results of approximate hand calculations for maximum stress and deflection at the middle span of the bridge, total mass of the bridge, and the vibration frequency of the bridge in current condition.

The bridge was idealized as a Generalized SDOF beam with fixed- support conditions. Therefore, the following equations were used for hand calculations:

30. Maximum stress at the middle of the bridge:

$$\sigma_{\max} = \frac{Mc}{I}$$

Where,  $\sigma_{\max}$  is the stress at the middle of the bridge (psi), M is the bending moment at the middle of the bridge (lb\*in), c is the distance from the neutral axis to the exterior fiber of the beam (in), and I is the moment of inertia of PSBBs (in<sup>4</sup>).

The 10 psi pressure load was converted to point load, P, at the middle of the bridge by multiplying it by the pressure area. The maximum moment at the middle of the span, and the moment of inertia of the PSBBs were calculated using the equations shown below.

$$P = 10 * (12 * 432) = 51840 \text{ lb}$$

$$M_{\max} = \frac{PL}{8}$$

$$M_{\max} = \frac{51840 * 1020}{8} = 6609600 \text{ lb.in}$$

$$I = \left( \frac{W_o H_o^3}{12} - \frac{W_i H_i^3}{12} \right) * n_b$$

Where,  $W_o$  is the box beam (PSBB) outside width (in),  $W_i$  is the box beam inside width (in),  $H_o$  is the box beam outside height (in),  $H_i$  is the box beam inside height (in), and  $n_b$  is the number of box beams.

$$I = \left( \frac{48 * 42^3}{12} - \frac{38 * 31.5^3}{12} \right) * 9 = 1776375.563 \text{ in}^4$$

$$\sigma_{\max} = \frac{6609600 * 21}{1776375.563} = 78.14 \text{ psi}$$

- Maximum deflection at the middle of the bridge:

$$\Delta_{\max} = \frac{PL^3}{192 EI}$$

$$\Delta_{\max} = \frac{51840 * 1020^3}{192 * 4496060.776 * 1776375.563}$$

$$\Delta_{\max} = 0.036 \text{ in.}$$

- Total mass of the bridge:

The total mass,  $m_t$ , of the bridge was calculated using its material and geometric properties as shown below.

$$m_t = \frac{[(W_o H_o - W_i H_i) L n_b + n_b W_o L t_w + W_i H_i t_d n_b n_d + 2W_i H_i t_e n_b] * w_c}{12^3 * 386.4}$$

Where,  $n_d$  is the number of diaphragms per box beam,  $t_d$  is the thickness of diaphragms (in),  $t_e$  is the thickness of box beam ends (in),  $t_w$  is the thickness of asphalt concrete wearing surface (in),  $w_c$  is the unit weight of concrete (lb/ft<sup>3</sup>).

$$m_t = \frac{((48 * 42 - 38 * 31.5) * 1020 * 9 + 9 * 48 * 1020 * 2.5) * 150}{12^3 * 386.4}$$

$$+ \frac{(38 * 31.5 * 18 * 9 * 3 + 2 * 38 * 31.5 * 18 * 9) * 150}{12^3 * 386.4}$$

$$= 2154.32 \frac{(\text{lb. s}^2)}{\text{in}}$$

- Vibration frequency of the bridge in current condition:

The frequency of the bridge  $f$  due to the vehicular loads was found by analyzing the collected data from the bridge and the ATB Bridge model using FFT algorithm. The average frequency for the bridge in current condition and for the ATB Bridge model was calculated as 3.4383 Hz and 5.4464 Hz respectively, and used to calculate the effective flexural rigidity of the bridge as shown below.

$$EI_{\text{Effective}} = \frac{f^2 * \pi^2 * L^3 * m_t}{126}$$

$$EI_{\text{Effective}} = \frac{3.4383^2 * \pi^2 * 1020^3 * 2193.1}{126} = 2.155140979 \text{ E12 lb. in}^2$$

$$EI_{\text{Effective}} = \frac{5.4464^2 * \pi^2 * 1020^3 * 2193.1}{126} = 5.407633111 \text{ E12 lb. in}^2$$

Modulus of elasticity of the bridge in current condition was calculated as shown below, and used to find the vibration frequency of the bridge in current condition using the FE frequency model.

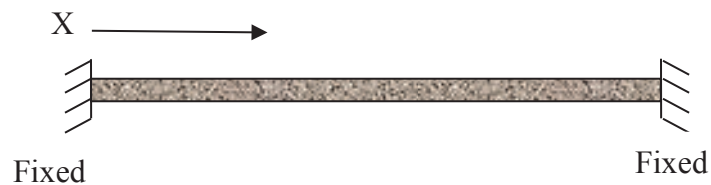
$$E = \frac{4496060.776 * 2.155140979 \text{ E12}}{5.407633111 \text{ E12}} = 1791845.827 \text{ psi}$$

## Appendix D

### Generalized Single Degree of Freedom Systems

To idealize a single span bridge as generalized SDOF system, it is necessary to assume a displacement configuration or shape function  $\varphi(x)$  that satisfies the beam kinematic and natural boundary conditions. The shape function derivation and the equations for estimating the load rating of a single span bridge with different boundary conditions are shown in this appendix.

1- Single span bridges with fixed-fixed supports.



$$\text{Vertical Displacement } Y(x, t) = \varphi(x) * \sin wt$$

Kinematic Boundary Conditions:

$$Y(0, t) = 0, \text{ and } Y(L, t) = 0$$

Natural Boundary Conditions:

$$Y'(0, t) = 0, \text{ and } Y'(L, t) = 0$$

$$Y(0, t) = 0, \text{ then } \varphi(0) * \sin wt = 0$$

$$\varphi(0) = 0$$

$$Y(L, t) = 0, \text{ then } \varphi(L) * \sin wt = 0$$

$$\varphi(L) = 0$$

$$Y'(0, t) = 0, \text{ then } \varphi'(0) * \sin wt = 0$$

$$\varphi'(0) = 0$$

$$Y'(L, t) = 0, \text{ then } \varphi'(L) * \sin wt = 0$$

$$\varphi'(L) = 0$$

$$\varphi(x) = a + bx + cx^2 + dx^3 + ex^4$$

$$\varphi'(x) = b + 2cx + 3dx^2 + 4ex^3$$

$$\varphi(0) = 0, \text{ then } a = 0$$

$$\varphi'(0) = 0, \text{ then } b = 0$$

$$\varphi'(0) = 0, \text{ then } cL^2 + dL^3 + eL^4 = 0$$

$$\varphi'(L) = 0, \text{ then } 2cL + 3dL^2 + 4eL^3 = 0$$

$$2c + 3dL = 4eL^2 = 0$$

$$\underline{- * (2c + 2dL + 2eL^2 = 0)}$$

$$dL + 2eL^2 = 0$$

$$\text{then } d = -2eL, \text{ and } c = eL^2$$

$$\varphi(x) = eL^2x^2 - 2eLx^3 + ex^4$$

$$\varphi(x) = eL^4 \left\{ \left(\frac{x}{L}\right)^2 - 2\left(\frac{x}{L}\right)^3 + \left(\frac{x}{L}\right)^4 \right\}$$



$$\varphi(x) = y_0 \left(\frac{x}{L}\right)^2 \left(1 - \frac{x}{L}\right)^2 \text{ Shape Function for Fixed – Fixed Beam}$$

$$M_e = \int_0^L m \{\varphi(x)\}^2 dx$$

$$K_e = \int_0^L EI \{\varphi''(x)\}^2 dx$$

$$\{\varphi(x)\}^2 = y_0^2 \left\{ \left(\frac{x}{L}\right)^4 - 4 \left(\frac{x}{L}\right)^5 + 6 \left(\frac{x}{L}\right)^6 - 4 \left(\frac{x}{L}\right)^7 + \left(\frac{x}{L}\right)^8 \right\}$$

$$\varphi''(x) = y_0 \left\{ 2 \left(\frac{1}{L^2}\right) - 12 \left(\frac{x}{L^3}\right) + 12 \left(\frac{x^2}{L^4}\right) \right\}$$

$$\{\varphi''(x)\}^2 = y_0^2 \left\{ 192 \left(\frac{x^2}{L^6}\right) - 288 \left(\frac{x^3}{L^7}\right) - 48 \left(\frac{x}{L^5}\right) + 4 \left(\frac{1}{L^4}\right) + 144 \left(\frac{x^4}{L^8}\right) \right\}$$

$$M_e = \int_0^L m y_0^2 \left\{ \left(\frac{x}{L}\right)^4 - 4 \left(\frac{x}{L}\right)^5 + 6 \left(\frac{x}{L}\right)^6 - 4 \left(\frac{x}{L}\right)^7 + \left(\frac{x}{L}\right)^8 \right\} dx$$

$$M_e = m y_0^2 \left\{ \frac{L^5}{5 L^4} - \frac{4 L^6}{6 L^5} + \frac{6 L^7}{7 L^6} - \frac{4 L^8}{8 L^7} + \frac{L^9}{9 L^8} \right\}$$

$$M_e = \frac{y_0^2 * m * L}{630} = \frac{y_0^2 * m_t}{630} =$$

$$K_e = \int_0^L EI y_0^2 \left\{ 192 \left(\frac{x^2}{L^6}\right) - 288 \left(\frac{x^3}{L^7}\right) - 48 \left(\frac{x}{L^5}\right) + 4 \left(\frac{1}{L^4}\right) + 144 \left(\frac{x^4}{L^8}\right) \right\} dx$$

$$K_e = EI y_0^2 \left\{ \frac{192 L^3}{3 L^6} - \frac{288 L^4}{4 L^7} - \frac{48 L^2}{2 L^5} + \frac{4 L}{L^4} + \frac{144 L^5}{5 L^8} \right\}$$

$$K_e = \frac{4 * EI * y_0^2}{5 * L^3}$$

$$F = \frac{1}{2\pi} \sqrt{\frac{K_e}{M_e}}$$

$$F = \frac{1}{2\pi} \sqrt{\frac{\frac{4 EI y_0^2}{5 L^3}}{\frac{y_0^2 m_t}{630}}}$$

$$\text{Effective Flexural Rigidity } EI_{\text{Effective}} = \frac{F^2 * \pi^2 * L^3 * m_t}{126}$$

$$\text{Beam Stiffness } K = \frac{192 * EI_{\text{Effective}}}{L^3}$$

$$P = K * \text{Deflection Limit}$$

$$DLFA = \frac{\text{acceleration amplitude for a vehicle at high speed}}{\text{acceleration amplitude for a vehicle at low speed}} \geq 1.33$$

$$\text{Bridge Capacity} = \frac{P}{DLFA}$$

2- Single span bridges with fixed-hinged supports.



$$\text{Vertical Displacement } Y(x, t) = \varphi(x) * \sin wt$$

Kinematic Boundary Conditions:

$$Y(0, t) = 0, \text{ and } Y(L, t) = 0$$

Natural Boundary Conditions:

$$Y''(0, t) = 0, \text{ and } Y'(L, t) = 0$$

$$Y(0, t) = 0, \text{ then } \varphi(0) * \sin wt = 0$$

$$\varphi(0) = 0$$

$$Y(L, t) = 0, \text{ then } \varphi(L) * \sin wt = 0$$

$$\varphi(L) = 0$$

$$Y''(0, t) = 0, \text{ then } \varphi''(0) * \sin wt = 0$$

$$\varphi''(0) = 0$$

$$Y'(L, t) = 0, \text{ then } \varphi'(L) * \sin wt = 0$$

$$\varphi'(L) = 0$$

$$\varphi(x) = a + bx + cx^2 + dx^3 + ex^4$$

$$\varphi'(x) = b + 2cx + 3dx^2 + 4ex^3$$

$$\varphi''(x) = 2c + 6dx + 12ex^2$$

$$\varphi(0) = 0, \text{ then } a = 0$$

$$\varphi''(0) = 0, \text{ then } c = 0$$

$$\varphi(L) = 0, \text{ then } bL + dL^3 + eL^4 = 0$$

$$\varphi'(L) = 0, \text{ then } b + 3dL^2 + 4eL^3 = 0$$

$$b + 3dL^2 + 4eL^3 = 0$$

$$\underline{-b - dL^2 - eL^3 = 0}$$

$$2dL^2 + 3eL^3 = 0$$

$$\text{then } d = -\frac{3eL}{2}, \text{ and } b = \frac{eL^3}{2}$$

$$\varphi(x) = \frac{eL^3}{2}x - \frac{3eL}{2}x^3 + ex^4$$

$$\varphi(x) = \frac{eL^4}{2} \left\{ \left(\frac{x}{L}\right) - 3\left(\frac{x}{L}\right)^3 + 2\left(\frac{x}{L}\right)^4 \right\}$$

$$\varphi(x) = y_0 \left\{ \left(\frac{x}{L}\right) - 3\left(\frac{x}{L}\right)^3 + 2\left(\frac{x}{L}\right)^4 \right\} \text{ Shape Function for Bin – Fixed Beam}$$

$$\{\varphi(x)\}^2 = y_0^2 \left\{ \left(\frac{x}{L}\right)^2 - 6\left(\frac{x}{L}\right)^4 + 4\left(\frac{x}{L}\right)^5 + 9\left(\frac{x}{L}\right)^6 - 12\left(\frac{x}{L}\right)^7 + 4\left(\frac{x}{L}\right)^8 \right\}$$

$$\varphi''(x) = y_0 \left\{ -18 \left(\frac{x}{L^3}\right) + 24 \left(\frac{x^2}{L^4}\right) \right\}$$

$$\{\varphi''(x)\}^2 = y_0^2 \left\{ 324 \left(\frac{x^2}{L^6}\right) - 468 \left(\frac{x^3}{L^7}\right) + 576 \left(\frac{x^4}{L^8}\right) \right\}$$

$$M_e = \int_0^L m \{\varphi(x)\}^2 dx$$

$$K_e = \int_0^L EI \{\varphi''(x)\}^2 dx$$

$$M_e = \int_0^L m y_0^2 \left\{ \left(\frac{x}{L}\right)^2 - 6 \left(\frac{x}{L}\right)^4 + 4 \left(\frac{x}{L}\right)^5 + 9 \left(\frac{x}{L}\right)^6 - 12 \left(\frac{x}{L}\right)^7 + 4 \left(\frac{x}{L}\right)^8 \right\} dx$$

$$M_e = m y_0^2 \left\{ \frac{L^3}{3 L^2} - \frac{6 L^5}{5 L^4} + \frac{4 L^6}{6 L^5} + \frac{9 L^7}{7 L^6} - \frac{12 L^8}{8 L^7} + \frac{4 L^9}{9 L^8} \right\}$$

$$M_e = \frac{y_0^2 * m * L}{33.15789474} = \frac{y_0^2 * m_t}{33.15789474} =$$

$$K_e = \int_0^L EI y_0^2 \left\{ 324 \left(\frac{x^2}{L^6}\right) - 468 \left(\frac{x^3}{L^7}\right) + 576 \left(\frac{x^4}{L^8}\right) \right\} dx$$

$$K_e = EI y_0^2 \left\{ \frac{324 L^3}{3 L^6} - \frac{468 L^4}{4 L^7} + \frac{576 L^5}{5 L^8} \right\}$$

$$K_e = \frac{7.2 * EI * y_0^2}{L^3}$$

$$F = \frac{1}{2\pi} \sqrt{\frac{K_e}{M_e}}$$

$$F = \frac{1}{2\pi} \sqrt{\frac{\frac{7.2 EI y_0^2}{L^3}}{\frac{y_0^2 m_t}{33.15789474}}}$$

$$\text{Effective Flexural Rigidity } EI_{\text{Effective}} = \frac{F^2 * \pi^2 * L^3 * m_t}{59.6842}$$

$$\text{Beam Stiffness } K = \frac{768 * EI_{\text{Effective}}}{7 * L^3}$$

$$P = K * \text{Deflection Limit}$$

$$DLFA = \frac{\text{acceleration amplitude for a vehicle at high speed}}{\text{acceleration amplitude for a vehicle at low speed}} \geq 1.33$$

$$\text{Bridge Capacity} = \frac{P}{DLFA}$$

3- Single span bridges with simply supported boundary conditions.



$$\text{Vertical Displacement } Y(x, t) = \varphi(x) * \sin \omega t$$

Kinematic Boundary Conditions:

$$Y(0, t) = 0, \text{ and } Y(L, t) = 0$$

Natural Boundary Conditions:

$$Y''(0, t) = 0, \text{ and } Y''(L, t) = 0$$

$$Y(0, t) = 0, \text{ then } \varphi(0) * \sin \omega t = 0$$

$$\varphi(0) = 0$$

$$Y(L, t) = 0, \text{ then } \varphi(L) * \sin \omega t = 0$$

$$\varphi(L) = 0$$

$$Y''(0, t) = 0, \text{ then } \varphi''(0) * \sin \omega t = 0$$

$$\varphi''(0) = 0$$

$$Y''(L, t) = 0, \text{ then } \varphi''(L) * \sin wt = 0$$

$$\varphi''(L) = 0$$

$$\text{Shape Function } \varphi(x) = y_0 \sin \frac{n\pi x}{L}$$

$$\varphi'(x) = \frac{\pi}{L} y_0 \cos \frac{n\pi x}{L}$$

$$\varphi''(x) = -\frac{\pi^2}{L^2} y_0 \sin \frac{n\pi x}{L}$$

$$\{\varphi(x)\}^2 = y_0^2 \sin^2 \frac{n\pi x}{L}$$

$$\{\varphi''(x)\}^2 = \frac{\pi^4}{L^4} y_0^2 \sin^2 \frac{n\pi x}{L}$$

$$M_e = \int_0^L M \{\varphi(x)\}^2 dx$$

$$K_e = \int_0^L EI \{\varphi''(x)\}^2 dx$$

$$M_e = \int_0^L m y_0^2 \sin^2 \frac{n\pi x}{L} dx$$

$$M_e = m y_0^2 \int_0^L \sin^2 \frac{n\pi x}{L} dx$$

$$M_e = \frac{m * L * y_0^2}{2} = \frac{m_t * y_0^2}{2}$$

$$K_e = \int_0^L EI \frac{\pi^4}{L^4} y_0^2 \sin^2 \frac{n\pi x}{L} dx$$

$$K_e = EI \frac{\pi^4}{L^4} y_0^2 \int_0^L \sin^2 \frac{n\pi x}{L} dx$$

$$K_e = \frac{\pi^4 * EI * y_0^2}{2 * L^3}$$

$$F = \frac{1}{2\pi} \sqrt{\frac{K_e}{M_e}}$$

$$F = \frac{1}{2\pi} \sqrt{\frac{\frac{\pi^4 EI y_0^2}{2 L^3}}{\frac{m_t * y_0^2}{2}}}$$

$$\text{Effective Flexural Rigidity } EI_{\text{Effective}} = \frac{4 * F^2 * L^3 * m_t}{\pi^2}$$

$$\text{Beam Stiffness } K = \frac{48 * EI_{\text{Effective}}}{L^3}$$

$$P = K * \text{Delection Limit}$$

$$DLFA = \frac{\text{acceleration amplitude for a vehicle at high speed}}{\text{acceleration amplitude for a vehicle at low speed}}$$

$$\text{Bridge Capacity} = \frac{P}{DLFA}$$